UNIVERSITÀ POLITECNICA DELLE MARCHE

FACOLTÀ DI INGEGNERIA

CORSO DI LAUREA MAGISTRALE IN BIOMEDICAL ENGINEERING

HYPERSPECTRAL IMAGING SYSTEM IN FORENSIC SCIENCE: BACKGROUND CORRECTION VIA NEURAL NETWORK

Relatore

Prof. LORENZO SCALISE

Tesi di Laurea di:

MARIA TERESA PUCARELLI

Correlatore

Prof. PAOLO CASTELLINI

ANNO ACCADEMICO 2020/2021

Abstract

In recent years Hyperspectral Imaging System (HIS) has seen many technological developments that have led Forensic Science to use this powerful tool for crime resolution. Hyperspectral Imaging System is very advantageous technique as it is fast, portable, non-destructive, and integrates conventional *spectroscopy* with *imaging*, allowing to have both the spectral and spatial information of an object. Of the various biological traces found at a crime scene, the blood is the most important *information carrier*, as it provides useful information for solving a crime. DNA analysis makes it possible to trace the suspect or victim, while the chronology of events can be reconstructed by estimating the age of the blood. Hemoglobin is the main *chromophore* of the blood, and its spectrum dominates the blood spectrum in the visible region allowing to identify its main features. However the blood spectrum is influenced by the substrate on which it is deposited. Texture and colors of the materials can affect the bloodstain and its spectrum, degrading it or blending with it, such as dark and red colors, unlike light colored materials on which the blood is visible to the naked eye.

This study aims to obtain a valid method for background correction, exploiting Multilayer Perceptron (MLP) neural network, generated through a Bayesian optimization approach. This new approach enables high performance background correction with a mean percentage error of 0.1% and a standard deviation of $\pm$ 0.05%.

INDEX

1 INTRODUCTION

Forensic science is defined as the application of the methods of the natural and physical sciences to matters of criminal and civil law [1]. In particular it is the application of scientific analysis in a legal context with the ultimate aim of solving crimes [2]. Forensic science is responsible for identifying, recognizing, individualizing and evaluating the different evidence found at a crime scene [3]. In order to solve crime several specialized skills and tools are used by crime scene investigators and lab technicians, allowing the collection and analysis of evidence [4]. Forensic science is evolving rapidly thanks to advancement of technological equipment, and recent scientific developments [2]. This is of fundamental importance, considering that analysis of forensic evidence is the key that allows to have information on the link between the victim and the suspect or between the suspect and the crime scene [2]. Forensic engineering is a part of forensic science which uses the concepts of chemical, mechanical, civil, and electrical engineering as tools in the reconstruction of crimes and the determination of their cause [1].

On the crime scenes it is possible to find several biological evidence of relevant importance in court investigations [5]. The most common and precious body fluid presents on forensic casework is the *blood*, defined as *information carrier* [6]. The blood is so precious because the analysis and age determination of the bloodstains could lead to the identification of the suspect or the victim [5]. Through the study of size and shape of the bloodstains it is possible to obtain information on the position and motion of suspect and victim [7]. While knowledge on the age of the bloodstains confirms or does not confirm the link between the blood and the crime scene, furthermore it gives information about the time when the crime was committed [8].

The first step to reconstruct crime scenes in forensic science is the identification of bloodstains, through the development of a technique that confirms the suspected traces as blood [5][9]. In fact, bloodstains can be confused with other substances due to the color and the appearance on different substrates [5]. In particular, some colors such as red or brown are very similar to the color of the blood, while dark substrates absorb a high quantity of incident light so that the contrast between the blood trace and the support is low [9]. These factors cause problems in identifying traces of blood through visual examination alone [9].

Once the blood trace has been identified, the DNA analysis can proceed leading to the identification of the suspect [5]. DNA analysis is expensive and time consuming so it should only be done on real blood traces, and for this reason the first important step in the analysis of forensic evidence is the identification of bloodstains [5].

Generally presumptive tests are used for bloodstains [10]. These tests include wet chemical methods based on the use of chemicals which in contact with the blood change color, fluoresce or luminesce [10]. Wet chemical tests, including Kastle–Meyer (KM), Leucomalachite Green (LMG), Benzidine, and Luminol, are sensitive to blood and quick [11]. However they are not specific to blood and can generate false positives, also due to the huge variety of substances and substrates [5][11]. In order to reduce false positives presumptive tests require a confirmatory test such as spectroscopic, chromatographic, microscopic, and crystal tests, but these methods require sample preparation or use chemical substances which could cause problems for subsequent analyzes, such as pattern and DNA analysis [5].

The Kastle-Meyer test belongs to the presumptive tests, also called phenolphthalein test because involves the use of phenolphthalein chemical [11]. This chemical will react with hydrogen peroxide in the presence of hemoglobin to produce a bright pink color [11]. KM test does not present high sensitivity to blood [5]. Leucomalachite green (LMG) is another presumptive test designed for field use; it is simple to use and the color change would appear within a few seconds with a sensitivity comparable to that of the KM test [5][11]. However, several experiments have shown that LMG test causes DNA damage, so samples after this type of test are not suitable for the DNA confirmatory biological test [11].

Luminol test is the most sensitive presumptive test [5]. It is based on the use of an alkaline solution of sodium carbonate and sodium perborate applied as a spray, which in the presence of blood produces a bluish luminescence that persists for seconds [11]. However, excessive spraying could lead to loss of detail, thereby damaging the blood sample tested [11]. Luminol test is more sensitive and produces fewer false positives compared to the KM test, but it requires a dark environment [5].

These tests are contact tests in the sense that they involve contact with the samples which can lead to the destruction of the sample itself and damage to the DNA [11]. Chemicals can lead to a loss of the bloodstain patterns, can interfere with subsequent tests, such as confirmatory test and DNA analysis, and can be harmful to the investigators [10].

Consequently the samples cannot be used for DNA analysis creating problems for the identification of the suspect or victim [11]. Therefore to discriminate the blood non-contact techniques are necessary, so non-destructive for the DNA and for the sample, simple and quick to use [11]. Non-contact techniques include several spectroscopic techniques such as Raman, reflectance, electron paramagnetic resonance (EPR), nuclear magnetic resonance (NMR), and infrared (IR) spectroscopy [5]. However, spectroscopy techniques are limited because they provide spectral information of the sample, but not spatial information of the area under observation, which is useful for extracting information from samples with different shapes on different backgrounds [5].

On the traces of blood identified it is also possible to carry out other analyzes in addition to DNA analysis. One of the fundamental objectives of forensic research is the reliable determination of the moment in which a crime was committed, and the knowledge on the age of the bloodstains allows to have this information [12]. The knowledge of the bloodstain aging allows to have the reconstruction of the timing of the event, the determination of the time of the victim's injury or death and the reduction of the number of suspects [12]. The time for blood stains is defined as the time elapsed since its creation [6].

Several methods have been investigated for the study of the age of the blood stains, like the degradation of RNA, atomic force microscopy, Electron Paramagnetic Resonance (EPR) , High-Performance Liquid Chromatography (HPLC) or the oxygen electrode based on the study of the changes that occur in the oxyhemoglobin-hemoglobin ratio of the blood stains [9][10]. However, these methods have not yet been implemented in forensic practice, and most require sample preparation and the need to be performed in a [10]. Since the color of a bloodstain changes from red to brown over time, optical methods could be used to quantify the color of blood stains and thus obtain information on the age of the blood [9]. The change in color is due to the effects that environmental variables have on the blood, and this has been studied using the reflectance spectra of the blood stains [9]. A non-destructive method for estimating the age of blood stains is based on the use of visible reflectance spectroscopy [8]. Visible reflectance spectroscopy can be used to determine the relative fractions of hemoglobin derivatives and to estimate the age of bloodstains by comparing the fractions with reference data [8]. The disadvantage of spectroscopy is that point measurements of suspected bloodstains require a lot of work and time, in addition to the fact that spectroscopy only provides spectral and non-spatial information [5][8].

The common solution that tends to solve the problems caused by the techniques used for blood identification and blood age determination is found in Hyper Spectral Imaging (HSI), as it is fast and non-destructive [6]. HSI was originally developed for remote sensing applications satellite imaging data of the Earth [13]. Over time it has found applications in numerous other fields, such as archeology and art conservation, biomedicine, the control of vegetation and water resources, mineralogy and geology, pharmaceuticals, food science and medical diagnosis [11][13][14].

HSI is also widely used in forensic practice the field on which this work focuses. Hyperspectral imaging is considered an important and powerful emerging tool for the analysis of forensic traces since it allows to detect, visualize and identify these traces also allowing to estimate their aging [13]. This technique integrates conventional *spectroscopy* and *imaging*, obtaining both *spectral* and *spatial* information of all samples of the inspected area; in this way the spectral properties of samples can be recorded together with information about their position in the scene [8]. Hyperspectral imaging is suitable for non-contact identification of blood traces as it limits contamination and destruction of traces [13]. The traces of blood can be identified thanks to the spectral differences that allow to obtain contrast between the trace and its background [13]. The individual spectra give information on the chemical composition of the sample useful for identification, and at the same time the spatial distribution of the bloodstain is recorded useful for observing its location on the scene [13]. The behavior of the spectra over time allows to obtain information on chemical changes within the sample useful for estimating the age of the blood, with the ultimate aim of reconstructing the chronology of events [13].

Hyperspectral imaging is a *reflection spectroscopy technique* and consequently provides information on the *reflectance spectrum* for each point of the sample examined [6].

The results obtained from HSI system are in the form of a "*hyperspectral cube*", also called *"hypercube"*, that is three-dimensional data composed of two spatial dimensions and one spectral dimension [6].

Recent technological developments have made the use of hyperspectral imaging in forensic investigations even more important [13]. The advantage of these systems is that they are fast and portable so that they can be transported to the crime scene where the traces are analyzed directly in situ, in the original context, thus avoiding the transport of the samples to the laboratory which could cause the loss of information of the sample itself [8]. In

addition, the development of rapid scanning systems allows to scan a complete scene [13]. In this way it is possible to reduce the workload in forensic laboratories with measurements that are fast, non-invasive, i.e. the samples are not touched, and the relevant information is provided to the investigators almost instantly [6].

In this work Hyperspectral imaging system is exploited to acquire hyperspectral cube of samples consisting of several substrates on which one blood drop is deposited. This work focuses on the relationship between bloodstains and substrates, as the substrate can influence the aspect of the blood. In fact, the materials have texture and colors that can affect the bloodstain and its spectrum, degrading it or blending with it, such as dark and red colors, unlike light colored materials on which the blood is visible to the naked eye. A substrate influences the blood spectrum because the colored background absorbs visible light disturbing the measured reflectance spectra of the bloodstains [15].

This thesis work aims to remove substrate contribution in the reflectance spectra of the blood drops deposited on substrate itself, exploiting Multi-Layer Perceptron (MLP) neural network. This model is generated through a Bayesian optimization technique which maximizes a loss function in order to obtain the best model parameters. The model takes as input the reflectance spectra of bloodstain on a generic substrate, and outputs are the spectra that the bloodstains would have on a reference substrate. Once the clean reflectance spectrum of the blood is achieved, other analysis such as the age estimation of bloodstain can be executed, by observing the behavior of the blood spectra over time.

STATE OF ART

The Hyperspectral imaging system is an advantageous technique used in forensic practice for identifying bloodstains and estimating the aging of bloodstains. This technique allows to carry out these analyzes in a non-contact and non-destructive way for the examined samples, as well as being fast and portable, as previously said. Several authors have studied the bloodstains by using this imaging system.

In [8] Edelman et al. exploited HSI for estimating the age of blood. Hyperspectral imaging system allowed the recording of visible reflectance spectra of bloodstains, in which the quantities of oxy-hemoglobin (HbO_2), met-hemoglobin (met-Hb) and hemichrome (HC) in the blood were derived, and used to estimate the age by comparing these derivatives with a reference dataset [8]. The result was an aging of the blood of 200 days with an absolute error increasing with age [8].

In [16] the age of bloodstains was determined non-destructively through linear discriminant analysis based on the changes of the absorption spectra over time, as over time the composition of the blood is altered. In this study, training and testing dataset were taken from the same blood, and this has resulted in a good age estimates with a high level of accuracy, while the accuracy decreases with the use of different bloodstains [16].

A similar method is used for the identification of bloodstains in [17] and [18].

For the identification of the blood was proposed a method based on Soret peak absorption in hemoglobin spectra as is possible to see in [19]. This methodology was confirmed also in [20] that indicated greater specificity and sensitivity for identification of the blood based on Soret peak, in [21] that used the Soret peak for the identification of blood fingerprints on white tiles, and in [22] that used the Soret peak for the identification of blood fingerprints on different colored tiles.

In [5] is shown a study based on the use of HSI for identification of blood. A total of 225 blood and non-blood drops (like Ketchup, red acrylic paint, rust acrylic paint, red nail polish, fake blood, red ink, and brown acrylic paint) were deposited on white cotton fabric, white tile, and PVC wall sheet, for experimental and validation purpose. The spectral range of the camera was set in the interval between 397nm and 1000nm, and the spectral features between 500nm and 700nm of the spectral range were considered [5]. There are some

studies aimed at identifying the blood using several substrates especially patterned and dark backgrounds, like in [23].

In [24] Bo Li et al. visible hyperspectral imaging is used for detection and identification of bloodstains on several colored substrates. This study based on visible absorption spectrum of hemoglobin, and the results show a good performance in the discrimination of bloodstains from other reddish stains [24].

Other methods can be used for the identification of bloodstains, as the method proposed in [25]. This study is based on the use of several neural network for the bloodstain classification, such as 1D, 2D, 3D convolutional neural networks (CNN), multilayer perceptron (MLP), and recurrent neural network (RNN). The dataset used are composed by several images with blood substances and non-blood substances, but that are similar to the blood such as ketchup, artificial blood, etc. [25]. Two types of experiments were conducted in this study. In the first experiment both training and test set derive from the same image and it is called Hyperspectral Transductive Classification (HTC), while in the second experiment, called Hyperspectral Inductive Classification (HIC), the test set derives from different image, for this reason it is more useful in the forensic investigators, but also more challenging for classifier [25]. The results of the transductive case show a comparative performance for all the neural network models, in particular the overall accuracy range is 98-100% for simple image set, and 74-94% for difficult image set, for all the models [25].

2 HYPERSPECTRAL IMAGING SYSTEM

Hyperspectral imaging is a reflection spectroscopy technique that integrates conventional *spectroscopy* and *imaging*, so that the spectral properties of an object are recorded together with information about its position, as previously reported.

HSI is able to measure the interaction between light and matter dependent on the light and optical properties of the sample, for this reason it is used to characterize the material, which means that the sample must be illuminated [13].

In this section a description of the electromagnetic spectrum, and of the phenomena that originate from the interaction of light with matter will be reported. Spectroscopy will be introduced with particular attention to reflectance spectroscopy, being HSI reflection spectroscopy technique. The fields of application of hyperspectral imaging will be described, in particular the forensic field which is the main theme of this work. Finally, a detailed description of the hyperspectral cube with its acquisition methods, the hyperspectral imaging system, and the calibration procedure of the system will be reported.

2.1 Electromagnetic spectrum

Hyperspectral imaging is a technology based on hyperspectral analysis, i.e. on a measurement process based on the visual representation of the *electromagnetic radiation* reflected by the *electromagnetic spectrum* [26]. An electromagnetic radiation originates from charges in motion which accelerate in matter, and it is defined as the transfer of energy in the form of *electromagnetic waves* and *photons* [27]. Thanks to its wave nature, an electromagnetic radiation can be classified according to the length of its waves, or the *wavelength*, thus defining different types of electromagnetic radiation [28] The organization of all the possible wavelengths that an electromagnetic radiation could have, from the shortest to the longest wavelength, define the electromagnetic spectrum; this wavelength range starts from zero and reaches almost infinity, and can be divided into various regions [27]. The term *light* is a synonym of electromagnetic radiation, which includes Gamma Rays, X-Rays, Ultraviolet, Visible, Infrared radiation, Microwave and Radio waves, the different regions of the electromagnetic spectrum; the division of light into regions can also be done according to the *frequency* of the electromagnetic radiation, and not only according to its wavelength [27]. It must be considered that there is a gradual

transition between one region and another, therefore this division of the spectrum is not completely correct [27].

The following table shows the different regions of the electromagnetic spectrum according to their relative wavelengths and frequencies.

Table I

Type of electromagnetic radiation	**Wavelength**	**Frequency**
Radio waves	10 km - 10 cm	≤ 250 MHz
Microwave	10 cm - 1 mm	250 MHz - 300 GHz
Infrared	1 mm - 700 nm	300 GHz - 428 THz
Visible	700 nm - 400 nm	4280 THz - 749 THz
Ultraviolet	400 nm - 10 nm	749 THz - 30 PHz
X-Rays	10 nm - 1 pm	30 PHz – 300 EHz
Gamma-Rays	≤ 1 pm	≥ 300 EHz

The electromagnetic radiation whose wavelength range goes from 400 nm to 700 nm is called *visible light*; these are the only wavelengths to which the human eye is able to respond visually [28]. Each wavelength of visible light is related to a specific color, in particular the visible spectrum is composed of three bands: Blue (400 nm - 500 nm), Green (500 nm - 600 nm) and Red (600 nm - 700 nm) [28]. The rest of the electromagnetic spectrum is made up of wavelengths not perceptible to the human eye: Gamma Rays, X-Rays and Ultraviolet radiation positioned before the Visible region because they have shorter wavelengths, while Infrared radiation, Microwaves and Radio waves are positioned after the Visible region because they have longer wavelengths [28].

In the following Figure 1 is shown the electromagnetic spectrum, and the wavelength range of the visible light.

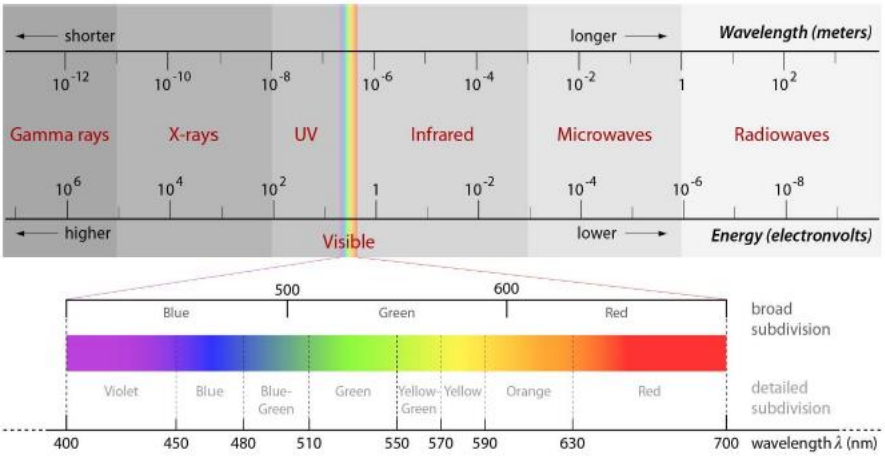

Figure 1: Electromagnetic spectrum [28].

2.2 Interaction of light with matter

Electromagnetic radiation (light) interacts with matter, composed of molecule, atoms and ions [27]. The phenomena that arise from this interaction depend on the relationship that links the wavelength (frequency) of the incident light with the physical size of the medium hit by the light [27]. The main phenomena caused by the interaction of light with matter are: *reflection*, *absorption* and *transmission*; for each wavelength the percentage of light reflected, absorbed and transmitted is equal to 100% [29]. When the electromagnetic radiation hits an object the first interaction occurs with the surface of the matter, a part of light energy is reflected by the surface itself [13]. There are two types of reflection depending on the characteristics of the surface: *specular reflection* and *diffuse reflection* [30]. Specular reflection is associated with light which is reflected from a smooth surface, such as a mirror with a well-defined angle, while diffuse reflection is associated with light that is reflected from a rough surface, which randomly reflects light in all directions regardless of the incidence angle [30]. The reflection depends on the difference of the refractive indices between the media, and it does not contains information from the inside of the medium [13]. Specular reflection and diffuse reflection are shown in Figure 2.

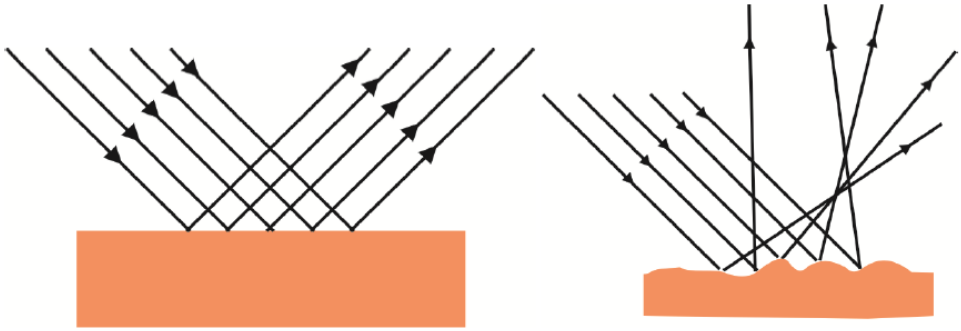

Figure 2: Specular reflection on the left, diffuse reflection on the right [30].

Within the matter part of the light energy is absorbed. Absorption depends on the molecules and atoms that make up the material [31].

Consider that the electrons in an atom exist in discrete energy levels (electron shells) and vibrate at a specific frequency, called the natural frequency [32]. If the light hitting the material has a frequency equal to that according to which the electrons are vibrating, the electrons will absorb energy from the light which will then be converted into a vibrational motion [32]. If the energy absorbed by the electron is equal to the difference in energy between two energy levels, the electron will move from the lower energy level (called 'ground' state) to the higher energy level; in this condition the electron is in an 'excited' state [32]. After the electrons have been excited they return to their original energy level, so move from the highest to the lowest energy level releasing energy in the form of heat or luminescence [13][32].

Absorption mechanism is shown in Figure 3.

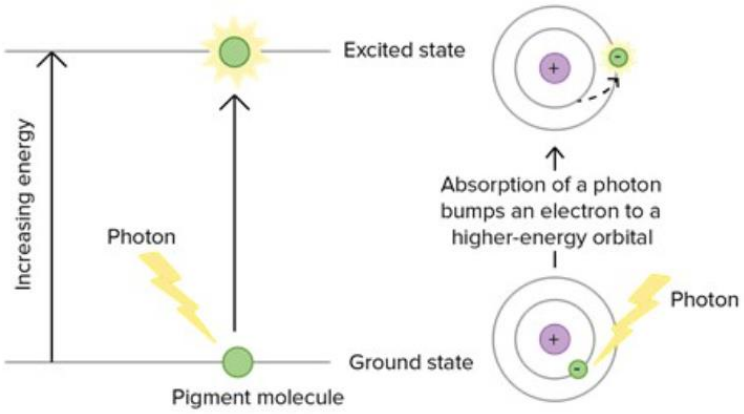

Figure 3: Absorption mechanism [32].

Finally some of the light energy is transmitted through the material; transmission does not occur for opaque materials which are therefore characterized only by absorption and reflection, unlike translucent materials which are characterized by reflection, transmission and absorption [29]. Inside the material, in addition to absorption, *scattering* could also occur [13]. Scattering is the process by which light interacts with the structures of matter, causing a change in the direction of propagation of light, which depends on its wavelength, the size of the particle, and the difference in the refractive indices of the media [13]. There are different types of scattering: *elastic scattering* in which the light is scattered at the same wavelength as the incident light, followed by diffuse reflection, and *inelastic scattering* in which the light is scattered in an inelastic way, causing wavelength shifts coinciding with the vibrational states of the molecules in the material, also called Raman scattering [13]. In Figure 4 are shown the different types of interaction between light and matter.

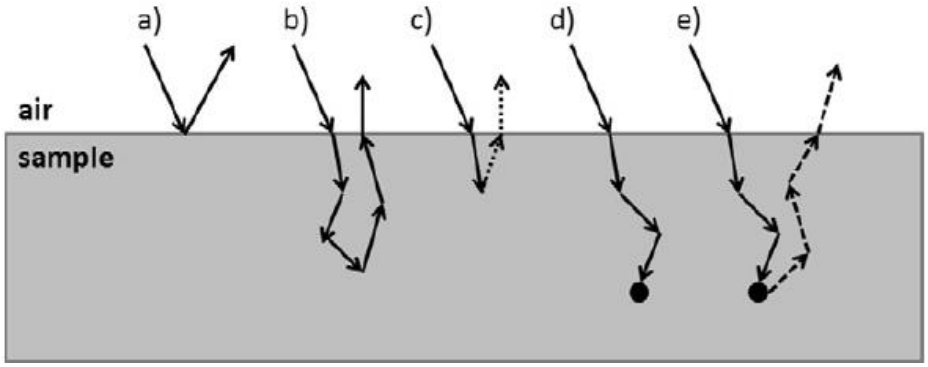

Figure 4: Types of interaction between light and matter: 1a) Reflection; 1b) Elastic Scattering followed by diffuse reflection; 1c) Inelastic Scattering followed by emission of Raman shifted light; 1d) Absorption; 1e) Absorption followed by photoluminescence emission [13].

2.3 Spectroscopy

Spectroscopy is the science based on the study of the interaction of electromagnetic energy with matter. This technique allows to characterize a material giving information on the elements it contains, and also on the quantity of these elements (spectrochemical). In addition to identifying the elements, spectroscopy provides important information from the atomic and molecular point of view of these elements (molecular spectroscopy) [33]. When light interacts with an object, part of the light is reflected and part is absorbed [34]. Of the amount of light absorbed, a part is emitted as light of a different wavelength or color [34]. In particular, spectroscopy studies both which and how much electromagnetic radiation is absorbed, and which and how much electromagnetic radiation is re-emitted [34]. The instrument used in spectroscopy is called a *spectrometer*, and the acquisitions that it provides are recordings of the absorbed and emitted light energy at specific wavelengths or specific frequencies [34]. These acquisitions are called *spectra*, and their role is to provide information of the substances on which the electromagnetic radiation is concentrated, information related to the atomic and molecular structure of the substance [34]. In particular the spectra allow to identify the unique characteristics of a substance, the so-called "fingerprints" [34].

Generally there are two types of spectra: *continuous* spectra and *discrete* spectra [35].

- Continuous spectra are characterized by light that is composed of a continuous range of different energies or colors [35]. The spectrum appears continuous as light is produced over a wide spectrum of wavelengths [35]. Generally these spectra are generated by solid objects or dense gases which, due to the generation of light, radiate heat [35].
- Discrete spectra are characterized by light which is made up of dark bands and luminous bands of different energies or colors; these spectra are caused by the atom [35]. Discrete spectra with dark bands are called *absorption spectra*, while discrete spectra with light bands are called *emission spectra* [35].

The different types of spectra are shown in Figure 5.

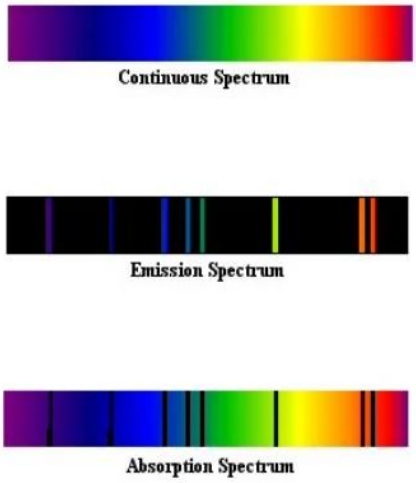

Figure 5: Different types of spectra [35].

Usually in spectroscopy two particular types of spectrum are considered: emission spectrum and absorption spectrum [34].

The *emission spectrum* is formed when light energy is emitted from a radiation source in specific regions of electromagnetic spectrum; its formation is due to a series of events [34]. The substance receives an incident electromagnetic radiation from an external source, absorbs energy to raise its atoms to higher energy levels, and finally when the excited atoms return to their previous levels it emits characteristic quantities of energy, thus defining the emission spectrum of substance [34].

The *absorption spectrum* is formed when part of light energy passing through a medium is absorbed by the medium itself, through internal energetic excitations, in specific regions of electromagnetic spectrum [34].

So the emitted light produces an emission spectrum, while the absorbed light produces an absorption spectrum. The energy of the emitted light is lower than the energy of the absorbed light [31].

In Figure 6 it is reported an absorption spectrum, which shows the absorbance as a function of the wavelength [31]. It is considered the *absorbance* since absorbance is the quantity that represents the quantity of light that is absorbed, while *absorption* describes the physical process [31]. The absorbance is on the vertical axis and has no unit of measure, the wavelength is on the x axis; peaks are defined as absorption lines or *absorption bands* [31].

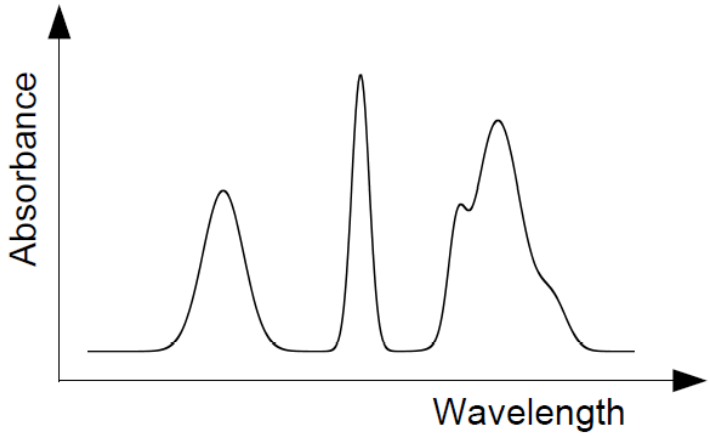

Figure 6: Absorption spectrum [31].

Starting from the definition of the absorption spectrum it is possible to define the *absorption spectroscopy*. Absorption spectroscopy is a particular type of molecular spectroscopy based on the study of the spectral characteristics of absorption of a material, at certain wavelengths, used to identify and quantify certain substances [36].

In addition to absorption spectroscopy there is another type of spectroscopy, called *reflectance spectroscopy*, based on reflection. Since Hyperspectral Imaging is a reflectance spectroscopy, it is useful to explain the main characteristics of a reflectance spectroscopy.

Generally reflectance spectroscopy is based on the study of the spectral characteristics of light energy that is reflected from a surface, and can be used for samples that are difficult to analyze with traditional methods [30]. With reflection spectroscopy, the absorption properties of a material can be extracted from the light reflected from the sample surface [30].

Diffuse reflectance spectroscopy (DRS) is the spectroscopy on which the present work focuses. In this regard, a *reflectance spectrum* is defined. The reflectance spectrum is formed when the energy of incident light on a surface is reflected in specific regions of the electromagnetic spectrum; it shows the *spectral reflectance* as a function of wavelength [37][38]. The spectral reflectance is given by the relationship between reflected energy and incident energy, and measures the quantity of light energy that is reflected by the sample [38]. In a spectral reflectance curve or reflectance spectrum the downward deflections

indicate the wavelength ranges for which the material absorbs the incident energy, and these deflections are called *absorption bands* [38].

Diffuse Reflectance Spectroscopy, also known as Elastic Scattering Spectroscopy, is a non-invasive technique based on the study of the spectral characteristics of a reflectance spectrum, obtained from the interaction of light with matter [39]. In this case the main interaction mechanisms are absorption and scattering, which vary with the wavelength producing the reflectance spectrum that will be recorded [39]. The information contained in this spectrum concerns the optical properties and the structure of the medium [39].

In particular, when light hits an object some of the light is reflected, scattered and transmitted [40]. The energy light that is detected by Diffuse Reflectance Spectroscopy is the back reflected, diffusely scattered light (of which a part is absorbed by the sample) [40].

2.4 Beer-Lambert law

Beer-Lambert law is an empirical relationship that correlates the quantity of light absorbed by a substance with the properties of this substance [41]. In particular the Beer-Lambert law is a linear relationship, that correlates the *absorbance* of a solution with the concentration, the molar absorption coefficient, and the optical coefficient of a solution [41]:

$$A = \varepsilon c l \tag{1}$$

where:

A= absorbance

ε = Molar absorption coefficient

c = Molar concentration

l = optical path length

This law affirms the existence of a linear relationship between the concentration and the absorbance of a solution, thus allowing to calculate the concentration of a solution starting

from the absorbance [41]. To understand this law it is necessary to explain what the *absorbance* of a solution is [41]. Consider a monochromatic light beam passing through a solution with an incident intensity I_0 and a transmitted intensity I [41]. With these two intensities it is possible to define the *transmittance* (T) of the solution as the ratio between the transmitted intensity and the incident intensity [41]:

$$T = \frac{I_0}{I} \quad (2)$$

The absorbance is linked to the transmittance and consequently to the transmitted intensity and incident intensity by the following relations [41]:

$$A = log_{10}\frac{I_0}{I} \quad (3)$$

where:
A= absorbance
I_0 = incident intensity
I = transmitted intensity

$$A = -log_{10}T \quad (4)$$

where:
A= absorbance
T = transmittance

Absorbance is a quantity without unit that describes the amount of light that is absorbed, differently from the absorption that describes the physical process, as previously mentioned [31]. Absorbance and transmittance are related by a logarithmic relationship: an absorbance of 0 corresponds to a transmittance of 100%, while an absorbance of 1 corresponds to a transmittance of 10% [41].

The reflectance spectra NIR can be converted into absorption spectra. This is made possible thanks to the following approximation [39]:

$$A = log_{10}\frac{1}{R} \quad (5)$$

where:

A= absorbance

R = reflectance; remembering that the reflectance is given by the relationship between reflected energy and incident energy, and measures the quantity of light energy that is reflected.

This means that the Beer-Lambert law is valid for NIR Diffuse Reflectance Spectroscopy. However there is a contradiction, since the Beer-Lambert law assumes that the diffusion and reflectance of the radiation are insignificant, but the use of the values obtained from this approximation works for the quantitative interpretation of the data [39].

2.5 Hyperspectral Imaging System in the forensic science

Hyperspectral imaging also called imaging spectrometer was originally developed for remote sensing applications of Earth satellite imaging, and has also been used for several applications by NASA [13][14]. Over time it has found applications in numerous other fields, such as archeology and art conservation, biomedicine, vegetation and water resources control, mineralogy and geology for the identification of precious gems or oil fields, pharmaceuticals, and food science [11][13][14]. Moreover, thanks to its imaging aspect, HSI has found great use in the medical diagnosis for the diagnosis of non-invasive pathologies and in surgical guidance [13][14]; its use is important for the identification of abnormal or diseased tissues and for early diagnosis of the disease [42].

Hyperspectral imaging is also widely used in forensic practice, since it is an important and powerful emerging tool for the analysis of forensic traces, in particular for the blood. The analysis of the bloodstains present at the scene of a crime allows both to identify the

bloodstain in order to trace the suspect or the victim, and to estimate the age of the blood in order to reconstruct the sequence of events, as previously reported.

Hyperspectral imaging is not only used for the bloodstain analysis, but also for other types of forensic traces including hair, firearm propellants, fibers, drugs, condoms, bruises, paints, dentin and inks [13]. Furthermore, hyperspectral imaging has been shown to be a very valid technique for imaging of latent fingermarks, and for detecting traces of material inside these prints. Latent fingermarks are a mixture of eccrine from the finger (mainly composed by amino acids, proteins and inorganic compound), and sebaceous deposits obtained from touching other parts of the body (mainly composed by fatty acid esters) [13]. The chemistry of these residues changes among people, and it shows an increase in the amount of sebaceous deposits with age [13]. The aim of fingermarks detection techniques is to create contrast between the details of latent fingermark ridge and the background on which it is found [13]. Hyperspectral imaging is used both on untreated latent fingermarks and treated latent fingermarks [13].

Several studies have been conducted for the detection of untreated latent fingermarks. In [43] Exline et al. used visible reflectance and photoluminescence hyperspectral imaging on materials like paper and plastic, and the resulting images were compared to the images resulting from the conventional forensic imaging techniques. Latent fingermarks were detected on plastic with both techniques, while HSI showed better contrast on paper [43].

For what concern treated fingermarks, they are treated with some chemicals in order to increase both the contrast with the background and the sensitivity. In [43] Exline et al. and in [44] Payne et al. used HSI to observe an higher contrast, and best visualization of treated fingermarks with respect traditional methods. The results confirm a better performance of HSI rather than traditional methods, mainly due to the suppression of a fluorescent background, so some little details are visible with HSI and not with traditional methods.

Other substances such as drugs can be detected with the use of HIS [13]. In [45] Kalasinsky et al. used infrared HSI to detect drugs in hairs. This study must be made only the interior portion of the hair, in order to distinguish the drugs that are ingested by the human from the drugs that come in contact with the external part of the hair [45].

2.6 Hyperspectral Imaging System: description of the technique

Hyperspectral imaging has an important advantage, because being a reflectance spectroscopy technique that integrate conventional imaging and conventional spectroscopy, it allows to have both spectral and spatial information of an analyzed object. This technique allow to obtain the reflectance spectra for each point of the analyzed sample. In addition, the measurements are fast, non-invasive, no sample preparation, and as this system can be portable the measurements can be made directly in the original context, avoiding the contamination of the sample, as previously said.

Hyperspectral camera can be applied in different region of the electromagnetic spectrum, such as visible, mid infrared, near infrared, short infrared and ultraviolet [13]. This allows to observe, through the pixel spectra of the image acquired, the interaction between the light and the molecules in the scene at any wavelength, and consequently determine the presence of particular traces [25]

The spectral features result from the electronic vibrational resonances in the visible range and ultraviolet range, and result from molecular vibrational resonances in the near infrared range [42]. The visible (VIS) and near infrared (NIR) together form the visible-near infrared (VNIR) with a wavelength range between 400nm – 1000nm [42].

2.6.1 Hyperspectral cube: description and acquisition

The results obtained from hyperspectral imaging system are in the form of three-dimensional data with two spatial dimensions (x, y) and one wavelength dimension (λ), defining the so-called *hypercube* [13]. The information provided by the hypercube are images for each wavelength (λ_i), and the possibility of obtaining a spectrum for each single pixel (x_j, y_k), as shown in Figure 7 [13]. However, information from all three dimensions cannot be obtained at the same time as the instruments capture two dimensions at a time [13]. Furthermore, it is possible to stack the two-dimensional data in sequence through a temporal scan in order to obtain a three-dimensional hypercube [13].

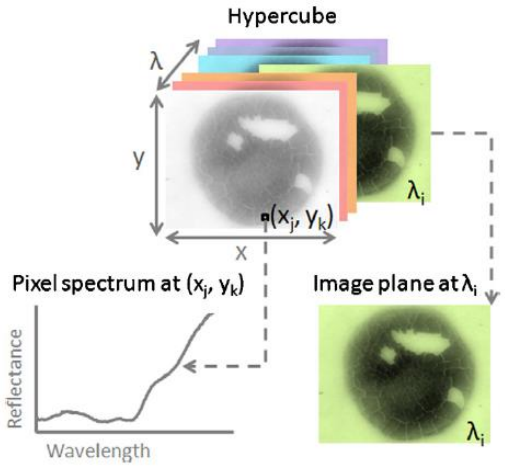

Figure 7: Hypercube of a bloodstain, with two spatial dimensions (x, y) and one wavelength dimension (λ). From the hypercube is possible to see an image plane for each wavelength (λi) and the spectrum for each pixel (x_j, y_k) [13].

Three methods can be defined for the acquisition of a three-dimensional hypercube: point scanning (or whiskbroom), line scanning (or pushbroom), and area scanning (or staredown) [13]. The names of these methods refer to the hardware used to acquire the hypercubes [13].

A *point scanning system* is based on the acquisition of a complete spectrum in a single point [13]. The acquisition takes place in the following way: the light arriving from this point enters the objective lens where it is separated into different wavelengths by a spectrometer, and finally detected by a linear matrix detector [13]. After having acquired and recorded the spectrum in this point, the same procedure is carried out in another point [13]. In order to obtain a complete hypercube this scan must be performed in both spatial directions [13]

In a *linear scanning system* the spectra of all the pixels belonging to a row of the image are acquired simultaneously. scattering light on a two-dimensional charge-coupled device (CCD) detector acquires a two-dimensional data matrix with a spatial dimension and spectral dimension [13]. The other spatial dimension of the hypercube is obtained by scanning the sample surface in a direction perpendicular to the imaging line [13]. This step implies a relative movement between the object and the detector, which is obtained by keeping the hyperspectral camera fixed and moving the sample with a conveyor belt or with a translation table, or by moving the camera and keeping the sample fixed [13].

In an *area scanning system* a two-dimensional data matrix is acquired, as in the previous case, but in this case the data represent an image with two spatial axes and not just a spatial axis [13]. Collecting a sequence of these images for one wavelength band at a time, a complete hypercube is obtained [13]. The wavelength of the incoming light is modulated with a tunable filter [13].

In Figure 8 are illustrates the three methods of acquiring a three-dimensional hypercube.

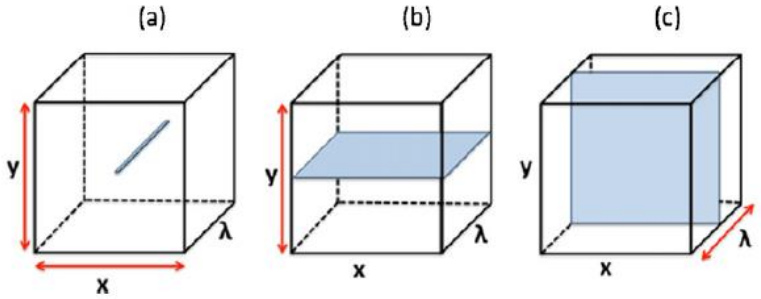

Figure 8: Acquisition methods of a three-dimensional hypercube: (a) point scanning system, (b) linear scanning system, and (c) area scanning system. Blue areas represent data acquired by one scan, while red arrows represent temporal scanning to complete the hypercube [13].

2.7 Hyperspectral Imaging System: description of the system

Hyperspectral imaging systems generally consist of several components: objective, wavelength modulator, detector, illumination and acquisition system, shown in Figure 9 [13].

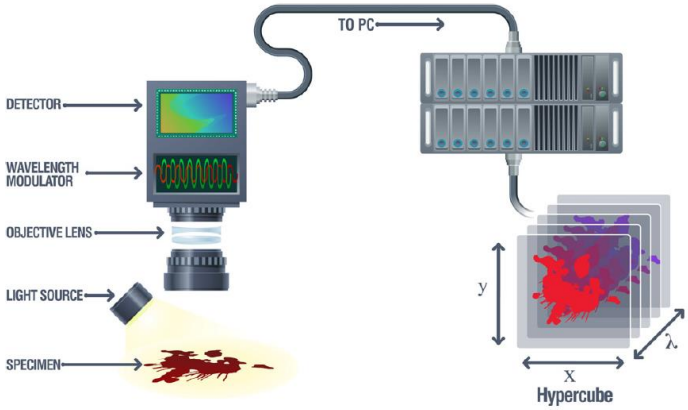

Figure 9: Schematic representation of the components of a Hyperspectral Imaging System, resulting in a hypercube of the sample [13].

It is important to consider that these components can be adapted to different application requirements, as forensic analysis can vary from laboratory conditions to field conditions, and areas of interest can vary from the microscopic level to landscapes [13].

The choice and position of the lighting system are of great importance for the reliability and performance of the entire hyperspectral system [13]. The choice is based on the type of lighting source, i.e. halogen, laser or LED lighting and on the choice of light properties, i.e. monochromatic light or broadband light [13]. Halogen lamps are broadband lighting sources usually used in the hyperspectral field [13]. These lamps can be supplied through an optical fiber or are used to directly illuminate the sample in question [13]. While in recent years the technology of light emitting diodes (LEDs) has had a strong development, which has led to having both broadband and narrowband light generators, thus providing a valid, economical, robust and reliable alternative to lighting halogen of the hyperspectral system [13]. Furthermore, the use of LED technology for hyperspectral imaging increases the advantage of having portable systems [13]. Finally, the laser can also be considered as a light source, which is a directional monochromatic light source, unlike broadband light sources [13]. For this reason they are particularly interesting for Raman and photoluminescence applications [13].

2.8 Calibration

A component of fundamental importance in the whole measurement system is the spectral and spatial calibration [13]. The raw data of a hypercube are not only due to the chemical composition of the sample but also take into account the intensity of the illumination, the transmission of the optics and the sensitivity of the detector [13]. For this reason spectral and spatial calibration is required in order to compensate for all this [13]. The calibration measurements usually performed for reflectance measurements are the acquisition of the system response in dark conditions and the acquisition of the system response to a uniform reference with high reflectance [13]. Acquiring the system response in dark conditions is done by covering the lens and dimming the light source [13].

However small variations may occur in the power supply sources, in the detector response, in the system alignment and in the lighting which can induce variations in the detected response, for this reason it is recommended to perform the calibration daily [13].

3 NEURAL NETWORK

Neural networks are a subgroup of machine learning, and are the heart of deep learning algorithms [46]. They are inspired by the neurons of the human brain and the way they work in transmitting signals [47]. Neural networks, non-parametric regression models, can capture any phenomena of any accuracy degree without prior knowledge of the phenomena [48].

In this study the neural network was used to differentiate the bloodstain in a material, and the Multilayer Perceptron (MLP) is the neural network used, so in this section the basic element of a neural network and the Multilayer Perceptron will be described .

3.1 Neural network function

Neural network, also called artificial neural network (ANN), is a computational *learning system* that differs from traditional computer for an important feature that characterizes it, the *learning* capability [49]. In fact a network can learn from its environment, and improve its performance through learning [49]. The learning is defined by Haykin as: "*Learning is a process by which the free parameters of a neural network are adapted through a process of stimulation by the environment in which the network is embedded. The type of learning is determined by the manner in which the parameter changes take place*" [50].

The idea of artificial neural network is based on human biology, in particular on the neurons of the human brain and on the way they work together to understand inputs from human senses [48][51]. Neural network uses a network of functions to translate a data input expressed in a form into a desired output generally expressed in another form [51]. They are organized in multiple layers, and each layer is composed by *artificial neurons* [47]. Generally, a neural network consists of one *input layer*, one or more *hidden layers* and one *output layer*, in which the artificial neurons can receive, process, and transmit signals to adjacent unit [47]. In fact the neurons in the layers are connected, and this means that the output of one neuron is the input of another neuron [47]. The information are transported similarly the synapses in the brain [47]. Neurons in the input layer do no processing, and no computation is performed in this layer as their neurons are used to provide inputs of the network [47][52]. Data input are send through the input layer to hidden layers, that process the data and extract the feature from them [47][52]. In finally

the processed data are treated and obtained through the output layer [47][52]. The good performance of a neural network depends on the number of layers used and not only as we will see later [47]. However there is no rule that establishes the right number of layers to be used to obtain good results, but a thumb rule shows that the minimum number of layers must be 2 [47].

Neural networks are one of the most important tool used in machine learning algorithms, and they are especially useful for classification and function approximation/mapping problems [48]. They are used to solve problems that are too complex to solve with conventional technologies, or in cases where the algorithmic solution does not exist, or in cases where the algorithmic solution is too difficult to find [48]. Machine learning algorithms that use neural network do not have to be programmed with specific rules to apply to the input data to produce the desired output (as for digital computers), but the neural network learning algorithm learns from processing of labeled examples building the rules itself, during a period that is called *training period* [51]. These labeled examples are data that belongs to the *training dataset*, i.e. data that is provided to the network to train it, so that the network sees and learns from this data. In addition to the training dataset, two other sets of data are considered: validation dataset and testing dataset [53]. *Validation dataset* is used to give an unbiased evaluation of a model fit on training data during the optimization of the model hyperparameters [53]. The network does not learn from this data, but the validation dataset is fed to the model so that the results are used by machine learning engineer to update the hyperparameters of the model [53]. *Test dataset* is the gold standard to evaluate the final model fit on training data. It is only used once the model is fully trained with training dataset and validation dataset [53].

Neural networks are suitable for the problems that people are able to solve but computers are not, as they are inspired by the human brain, for example pattern recognition and forecasting [48]. The difference between networks and the human brain is that networks are not affected by factors such as fatigue, emotional states and working conditions [48].

Today neural network can be applied to different field such as pattern classification/recognition, predictive analysis, signal processing, image processing, system modeling and identification, medical diagnosis and biochemical analysis [48][49]. In Figure 10 is illustrated a simple neural network.

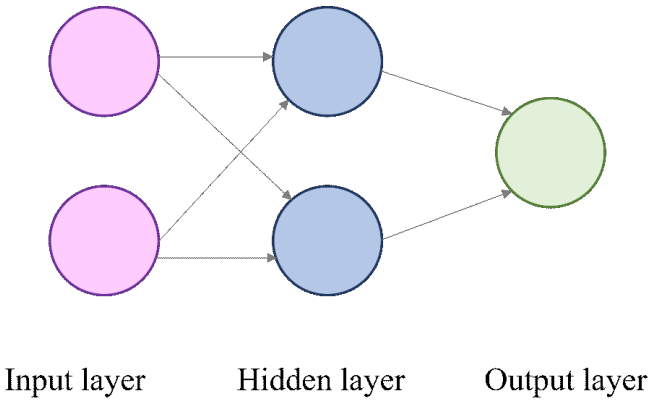

Figure 10: Simple neural network.

3.1.1 The biological neuron

The biological neuron is the functional unit of the nervous system and its function is to receive, process, and transmit information [54]. Generally, neurons are composed by three elements: *cell body* also called soma and two neural processes, *dendrite* and *axon*, that extend from cell body [54]. The neuron presents many dendrites that branch from the cell body and that receive input from other neurons at specialized junctions called *synapses*, while the axon which is generally one comes off the cell body and sends information, in the form of electrical signal called *action potential*, to other neurons through its axon terminals [54]. Sometimes the axons can branch sending information to more than one neuron, and these branches are called *collaterals* [54]. The neuron that sends information is called *presynaptic neuron*, and the neuron that receives information is called *postsynaptic neuron* [54]. Action potential is an event characterized by brief and large changes in membrane potential, in which the inside of the cell became positively charged with respect the outside [54]. This change in the membrane potential is called cellular depolarization and is due to an external stimulus [54]. The action potential follows the *all-or-none principle*, this means that the action potential is generated only if the cellular depolarization exceeds a threshold of about -70 mV, and the action potential generated is always the same, while if the cellular depolarization does not exceed the threshold the action potential is not generated [54]. Dendrite tree of a neuron is connected to thousand neurons, and when one of these neurons fire, generating an action potential, one of the dendrites receives negative or positive charge [54]. All the charges that arrive to the dendrites, and so to the cell body of the neuron, are summed in a process called temporal

and spatial summation [54]. The result is that some neurons are characterized by an inhibitory effect preventing the firing, and other neurons are characterized by an excitatory effect promoting the firing [54]. The Figure 11 illustrates the typical structure of a neuron.

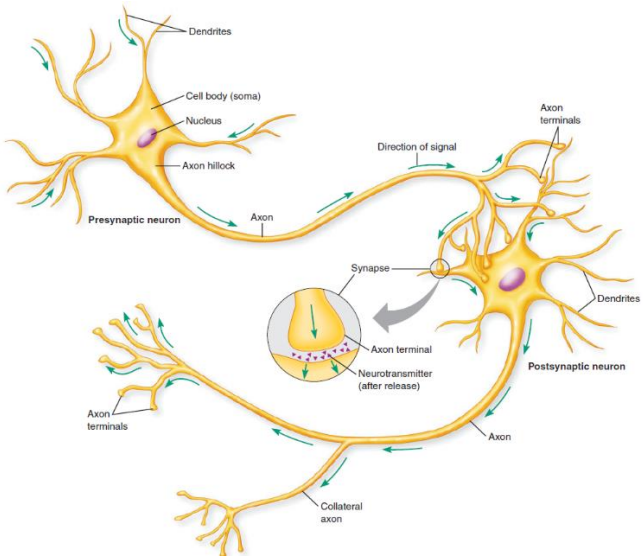

Figure 11: Structure of a typical neuron: communication between presynaptic neuron and postsynaptic neuron is shown [54].

3.1.2 The key element of neural networks

The artificial neuron also called *node* is the key element of any neural network, and the connection between these neurons forming a network [55].

The artificial neuron is a *simple processing unit* which takes one or more inputs and produces an output, and it is represented by a mathematical function [48][56].

In artificial neural networks, neurons communicate via synapses as it occurs in the brain. In this case, the synapses are modelled by a number called *weight* that can be positive or negative [57]. Each neuron receives weighted information from the neurons to which it is connected through these synaptic connections [57]. In particular the effect of each synapse is represented by the multiplication between the input signal and respective weight value (respective synapse of the neuron), while excitatory and inhibitory actions are modelled using positive weights and negative weights respectively [57]. So at every input is associated a weight which modifies the strength of the input itself [56]. Furthermore, each product is the analogue of a post-synaptic potential, and could be positive or negative according the sign of the weight [57].

The input ‘x’ and the weight ‘w’ are vector, in particular $x \in R^n$ and $w \in R^n$ with $n \in N$, that corresponds to the dimension of the input [55].

Inside the node the weighted inputs (PSPs) are summed together by arithmetic addition in order to obtain a linear function [57]. The artificial neuron adds to this weighted sum also another element called *bias* ‘b’, and the linear function obtained is the input signal of the *activation function* ‘*f* ’ of the node which determines the output ‘y’, according to equation (6) [55] [58]:

$$y = f(\sum_i x_i w_i + b) \quad (6)$$

The bias is a scalar element with an imaginary input of 1, that helps to correct some patterns in the data, but it is not always present [55]. It simply serves to compensate for the result of the activation function and so to shift its value [52].

The activation function is present in each node (of the hidden and output layers), and it transforms the input signal into an output signal, which in turn is used as input for adjacent neuron or is the final output of the network [47]. It is used to map the input to the output, and it helps the network to learn and recognize complex mappings from data [47]. Furthermore, the activation function limits the amplitude of the output of a neuron and determines if a neuron should be activated or not [48][58]. In particular it governs the threshold at which the neuron is activated, and the strength of the output signal [59]. The activation function can be linear or non-linear, and it is chosen according to the type of the problem to solve [58]. Moreover, non-linear activation function are chosen in order to add non-linearity to the neuron role [47]. This means that the activation function must make the network dynamic, and must guarantee the ability to extract complex information from data [47]. In fact, a neural network without an activation function is characterized by an output which is a simple linear function, i.e. polynomial of degree one (weighted sum) [47]. This function is simple to solve but cannot learn and recognize complex mappings from data because its complexity is limited [47]. The activation function is necessary otherwise the neural network acts as a Linear Regression Model with limited power and performance [47]. By using the non-linear activation function the network is able to obtain non-linear mappings from inputs to outputs and can perform very complicated tasks [47]. An

important feature of the activation function is the *differentiability*, which allows to implement the backpropagation optimization in order to calculate the errors with respect to the weights, and eventually optimize the weights with an optimization technique to reduce errors, such as Gradient Descend, this will be explained later [47].

There are different types of activation functions, and the prediction accuracy of a neural network is determined by the activation function used [47]. Activation functions commonly used in neural networks are: binary step function, linear activation function, sigmoid activation function, tanh activation function and ReLU activation function [47].

The schematic representation of an artificial neuron is shown in Figure 12.

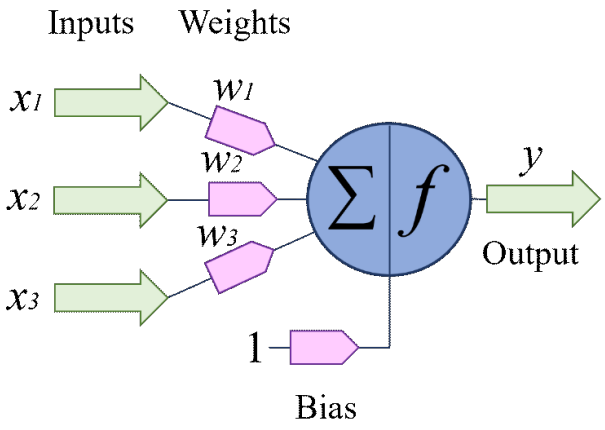

Figure 12: Schematic representation of an artificial neuron.

3.1.3 Training methods

Machine learning algorithms that use neural networks learns from processing of labeled examples building the rules itself, differently from the algorithm in the digital computers that have to be programmed with specific rules to apply to the input to obtain the desired output [51]. The period during which the learning algorithm that use neural networks learns from labeled examples is called *training period* [51]. The learning algorithm of a neural network can either be supervised and unsupervised [60].

Supervised training is based on the use of labeled datasets that are designed to train the neural network [61]. In supervised training, both data inputs and data outputs are provided in order that the network learns which are the features of the inputs required to obtain the desired output [51]. After analyzing several examples, the neural network starts to

elaborate new inputs and to produce accurate outputs [51]. The greater the number of examples given, the better the accuracy of the outputs obtained [51]. The outputs resulting from the network are compared with the desired outputs allowing the determination of an error, that will be used to adjust the weights which control network [60].

Unsupervised training is based on the use of data inputs without desired data outputs. In this case, it is the network itself that decides which features it will use to group the input data. This condition is called self-organization or adaption [60].

3.2 Multilayer perceptron

A Multilayer Perceptron (MLP) is a neural network in which series of nodes are stacked in a row and piled in different layers, and is characterized by one input layer, one or more hidden layers, and one output layer [52][62]. Perceptron represents one single neuron and is the basic element of a MLP. The Multilayer Perceptron was developed to overcome a limit of the Perceptron, as the Perceptron is a single neuron and cannot be applied to non-linear data. Furthermore, while in the Perceptron the neuron has an activation function that imposes a threshold such as sigmoid function or ReLU, in a Multilayer Perceptron can be used any arbitrary activation function [63].

The architecture of a MLP is *feedforward,* in the sense that the information are passed in forward direction starting from the input layer, passing through the series of hidden layers and arriving to the output layer [52]. This model architecture is able to predict new continuous outputs from new statistically independent input data starting from a set of continuous input-output variables [58].

The Multilayer Perceptron is trained by means of a *backpropagation algorithm*, a supervised learning technique, this means that both input data and output data are provided to the network [62]. Each neuron in the network processes the input data layer by layer until a result is obtained by the output layer [64]. The Multilayer Perceptron through the backpropagation algorithm adjust iteratively the weights (randomly initialized) with the aim to reduce the error of the model [64]. The *loss function* is the multivariable error function of the network, that determines the error of the model to understand the performance level of a neural network for certain tasks [48].

The error value is backpropagated from the output layer, through the neurons of the hidden layer in order to gradually adjust the weights until the correct output is produced [64]. The weights are updated based on how much they contributed to the error [64]. Updating the weights in this way allows the network to understand how to produce the correct output for this particular data input, thus the network learns [64].

This network uses a *stochastic gradient descent optimization algorithms* to change the parameter of the model, such as weights and learning rate, in order to reduce the error and increase model performance [65].

4 BLOOD

The blood is the body fluid analyzed in this study. As previously mentioned, the blood is considered the most precious body fluid on the crime scene, as the analysis and age determination of the bloodstains could lead to the identification of the suspect or the victim. The identification of bloodstains is the first step to follow, since that the blood can be confused with other substances. Once the blood traces have been identified, the blood can be analyzed, knowing for example its age. Aging of bloodstains confirms or not the link between the blood and the crime scene, and it also gives information about the time when the crime was committed.

This section will deal with the description of blood from an anatomical and physiological point of view. In addition, a detailed description of hemoglobin and of the spectral features of the blood will be reported, in order to understand how to identify blood and have information on its aging

4.1 Blood: anatomy and physiology

Blood is made up of a liquid component called *plasma* that transport hormones, proteins, waste products, electrolytes and organic nutrients, and a *cellular* component, shown in figure 13 [54]. The cellular component includes *erythrocytes* (red blood cells) which transport oxygen and carbon dioxide, *leukocytes* (white blood cells) which defend the body against pathogens, and *platelets* (cell fragments) which are fundamental in the formation of blood clots to prevent the loss of blood [54]. The cellular component of the blood is shown in Figure 13.

Figure 13: Cellular component of the blood [54].

In a healthy adult the total volume of blood is about 5.5 liters composed of erythrocytes (2.5 liters) and mainly plasma (3 liters), but also includes leukocytes and platelets [54].

Hematocrit is defined as the fractional contribution of erythrocytes to the blood, and is obtained by centrifuging a blood sample in a test tube, as shown in Figure 14 [54]. With centrifugation it is possible to observe the different components of the blood because when the blood is centrifuged its elements separate according to their density [54]. The erythrocytes are distributed on the bottom being denser than the other elements, the less dense is the plasma that stays at the top, and between these two lies there is a thin layer of leukocytes and platelets, called *buffy* [54]. The hematocrit gives information on the relative concentration of erythrocytes in the blood [54]. A low hematocrit indicates a lower than normal concentration of red blood cells, while a high hematocrit indicates a higher than normal concentration of red blood cells [54].

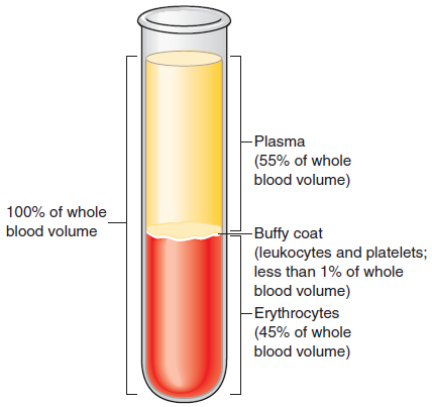

Figure 14: Determination of hematocrit [54].

4.1.1 Plasma

Plasma is an aqueous solution in which several solutes are dissolved, including proteins, nutrients (glucose, lipids and amino acids), waste products (urea and lactic acid), gas (oxygen and carbon dioxide), and electrolytes (sodium and potassium) [54]. The role of the plasma is to transport these solutes [54]. Plasma proteins are classified into albumins, globulins and fibrinogen [54]. Serum is the plasma from which fibrinogen and other coagulation proteins have been removed [54].

4.1.2 Leukocytes

Leukocytes, also called white blood cells, are the only functional blood cells being nucleated and with the cellular apparatus [54]. Unlike red blood cells, white blood cells thanks to their mobility are present in other tissues of the body and not only in the bloodstream [54]. The number of leukocytes in the blood is lower than that of erythrocytes, 4000–10,000 per cubic millimeter of blood [54]. Their function is to defend the organism from pathogenic microorganisms and foreign materials [54]. Leukocytes are classified into *granulocytes* and *agranulocytes* [54]. Granulocytes include neutrophils, eosinophils and basophils so called because they have protein-containing vesicles, while agranulocytes include monocytes and lymphocytes so called because they have no vesicles [54].

4.1.3 Platelets

Platelets are the smallest elements in the blood responsible for the events that induce the formation of blood clots, present in a number between 100,000 and 500,000 [54]. They contain the smooth endoplasmic reticulum, mitochondria and cytoplasmic granules but not the nucleus [54]. Platelets form when megakaryocytes, large portions of bone marrow cells, break off [54].

4.1.4 Erythrocytes

Erythrocytes, also called red blood cells, are the most abundant cells in the blood, 5 million per cubic millimeter of blood [54]. Their shape is like that of a disc with a diameter of 7.5 μm and a thickness of about 2 μm as shown in Figure 15 [54]. The main function of erythrocytes is to transport oxygen and carbon dioxide in the blood [54]. This transport allows the cells to receive oxygen from the lungs, and the lungs to receive carbon dioxide from the cells through which it is eliminated from the body [54]. The red blood cell is able to carry out this transport since it contains important proteins: *hemoglobin* and *carbonic anhydrase* [54]. Hemoglobin is responsible for the transport of oxygen and carbon dioxide, while carbonic anhydrase is responsible only for the transport of carbon dioxide [54].

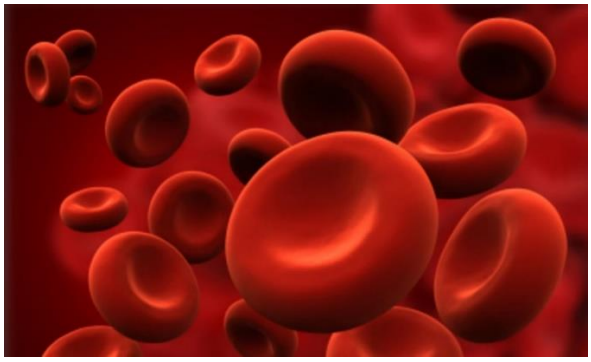

Figure 15: Red cells [54].

Hemoglobin is the most abundant protein found in red blood cells with more than 250 million molecules of hemoglobin per erythrocyte [54]. The function of hemoglobin is to transport oxygen from the lungs to the cells, and carbon dioxide from the tissues to the lungs from which it is eliminated [54]. For this reason it is defined as *two-way respiratory carrier* [54][66]. However, hemoglobin has a greater affinity for oxygen than for carbon dioxide [54]. It is composed of four polypeptide chains, two *alpha* chains and two *beta* chains, each of which has a *heme group* that is an iron-containing ring structure [54]. Iron is in its ferrous form giving the red blood cells a red color and therefore the blood a red color [54]. Each hemoglobin molecule can bind four oxygens thanks to the four heme groups, while carbon dioxide reversibly binds to the amino acids of the polypeptide chains [54]. Hemoglobin molecule and its heme group are shown in Figure 16.

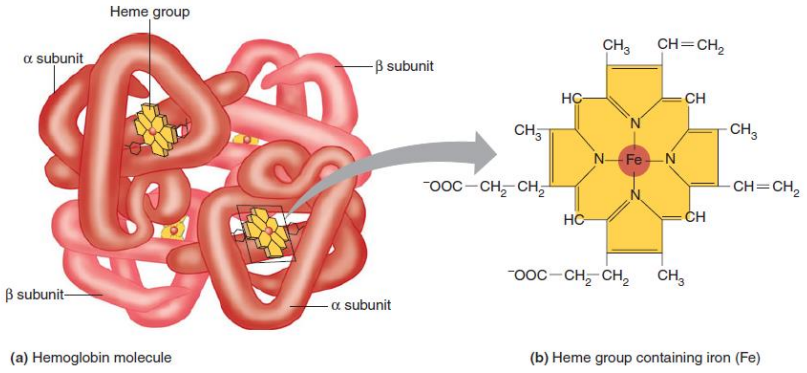

Figure 16: (a) Hemoglobin molecule composed of two alpha chains and two beta chains. (b)Chemical structure of a heme group [54].

The main chromophore of the blood is hemoglobin since it constitutes 97% of the dry content of the blood [67]. Hemoglobin can be present in several forms called *hemoglobin derivatives* [68]. Within the human body hemoglobin is present in two forms: one form without oxygen called *de-oxyhemoglobin* (Hb) and one form saturated with oxygen called *oxyhemoglobin* (HbO_2) [68]. A small percentage of oxyhemoglobin, about 1%, is auto-oxidized into another form called *methemoglobin* (met-Hb), which in turn is reduced to de-oxyhemoglobin by the cytochrome b5 reductase protein [68]. Once out of the body the blood in contact with oxygen completely saturates to oxyhemoglobin [68]. However, the cytochrome b5 is present in less quantity, therefore the transition of oxyhemoglobin in methemoglobin will no longer be inverted [68]. After hemoglobin auto-oxidizes to met-Hb, it is denatured to hemichrome (HC) [68]. In Figure 17 is illustrated the schematic representation of hemoglobin degradation.

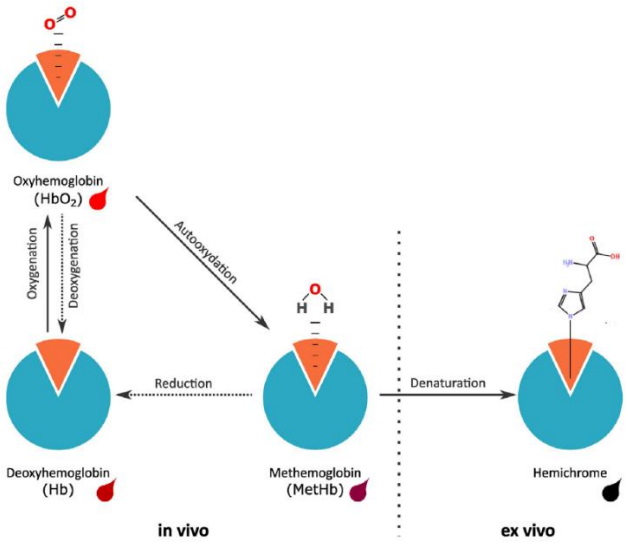

Figure 17: Schematic representation of hemoglobin degradation: hemoglobin peptide chain (blue), bound heme group(orange). Oxy-hemoglobin autoxidation into met-hemoglobin (from bivalent into trivalent iron that is irreversible ex vivo). Out of the body, the met-hemoglobin denatures in hemichrome [7].

The transition of HbO2, into met-Hb and into HC is accompanied by a change in the color of the blood from deep red to dark brown, due to the change in the concentration ratio of hemoglobin, and its derivatives (HbO_2, met-Hb, and HC) [68]. For this reason the absorption spectra of HbO2, met-Hb and HC are different from each other as shown in

Figure 18 [68]. Hemoglobin reflectance spectrum dominates the spectrum of a bloodstain in the visible region [9].

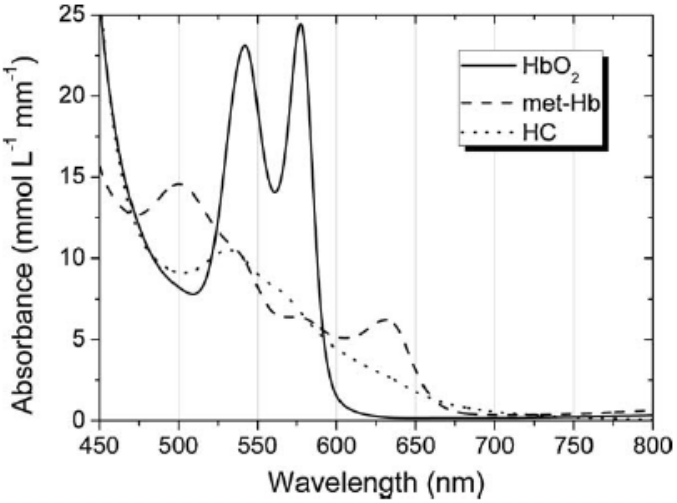

Figure 18: Absorption spectra of the three hemoglobin derivatives taken from [68].

Spectral features of the blood can be used both to identify blood, in order to distinguish blood from other substances that could be similar in appearance or color, and for estimating the age of the blood.

In a fresh bloodstain hemoglobin the absorbance spectrum of the blood is dominated by the oxyhemoglobin spectrum due to the fact that in fresh blood, outside the body, hemoglobin exists as oxyhemoglobin [69].

All the spectra of the hemoglobin derivatives present an intense absorption peak between 400 and 425nm, generally at 415nm, due to hemoglobin and called Soret peak [7]. The red color of the blood is due to Soret band, since it absorbs in the blue of the visible spectrum between 400 and 500 nm and reflects in the red of the visible spectrum [68]. There are also other red substances that absorb in the blue region of the visible spectrum, but the bandwidth is wider and not centered at 415 nm [68]. However Soret peak is not present in all substrates and depends on the lighting conditions [11].

The spectrum of oxyhemoglobin presents two smaller and wider absorption peaks than the Soret peak, between 500nm and 600nm: β peak at wavelength of 540 nm and α peak at

wavelength of 576 nm [7]. The spectrum of methemoglobin is characterized by peaks at 499nm and 626nm, while the spectrum of hemicrome shows a typical peak at 537nm [7].
Over the time, with the aging process, the blood spectrum will show several alterations between 400 and 640nm due to the change in the concentration ratios [7].
In details, it is possible to have information on blood aging according to:

- the decrease of α and β peaks, due to the autoxidation of oxyhemoglobin into meth-hemoglobin, followed by denaturation into hemichrome [69].
- the increase of methemoglobin absorption peaks [7].
- the decrease of the steepness of the curve between 600-650 nm caused by the formation of methemoglobin and hemichrome [5].

5 MATERIALS AND METHODS

In this study Hyperspectral imaging system is used to perform a series of acquisitions on several substrate on which are present bloodstains. Hyperspectral camera gives the possibility of obtaining a reflectance spectrum for each single point of the analyzed sample.

This work aims to remove the substrate contribution in the spectrum of the blood drop deposited on this substrate, by using a neural network. However, before doing this it is necessary to obtain the data (reflectance spectra) to be given to the network.

Three preliminary tests were performed to define the correct test bench, and the sample preparation. The first two preliminary tests led to the definition of the test bench, but also to the preparation of the sample, while the third test led to the optimal definition of sample preparation.

The part of the work relating to the definition of the test bench and sample preparation was carried out in collaboration with Delia Iafelice, for her thesis entitled "*Hyperspectral imaging in forensic science: definition of the test bench and age estimation of bloodstains on different substrates*". While the part of the work relating to the use of neural network, and the analysis of the obtained corrected spectra was carried out by me for this thesis work.

In this study the preliminary tests will be briefly described, while the test bench, the whole procedure followed to extract the data, and the use of neural network will be described more in detail. The detailed description of the preliminary tests can be found in Delia Iafelice's thesis entitled "*Hyperspectral imaging in forensic science: definition of the test bench and age estimation of bloodstains on different substrates*" .

5.1 Preliminary tests

The three preliminary tests are based on the use of the same Hyperspectral camera, and its scan angle is perpendicular to the acquired samples.

The source of illumination chosen is a halogen lamp that provides a better contribution to high wavelengths than to low ones, in particular between 480 nm and 1000 nm.

First preliminary test was performed with the use of four halogen lamps symmetrically fixed on the hyperspectral camera so as to be perpendicular to the analyzed sample, and

with the environmental light (fluorescent lamp) turned on. A drop of blood with anticoagulant EDTA was deposited simultaneously on 23 samples, but the acquisition was done individually for each sample, for previously established times. The calibration procedure, i.e. the acquisition of white and dark references, was performed once before the acquisitions of all the samples. The spectral range considered is the maximum offered by the camera between 400 nm and 1000 nm.

Second preliminary test was carried out with the use of two halogen lamps symmetrically fixed on the hyperspectral camera, so as to be perpendicular to the analyzed sample, and with the environmental light (fluorescent light) turned on. A drop of blood with EDTA was deposited on 15 samples with a time interval of 5 minutes, and the acquisition was done individually for each sample, for previously established times. The calibration procedure, i.e. the acquisition of white and dark references, was performed once before the acquisition of all the samples. The spectral range considered is the maximum offered by the camera between 400 nm and 1000 nm.

The third preliminary test was performed to determine where to properly deposit the blood drop on the substrate, since it was decided to place multiple samples on the same support in order to make multiple acquisitions at the same time. For this reason, two drops of blood were deposited on four sample chosen at random. In particular one drop was deposited on the external margin of the samples, and the other one was deposited on the inner margin of the samples, as shown in Figure 19.

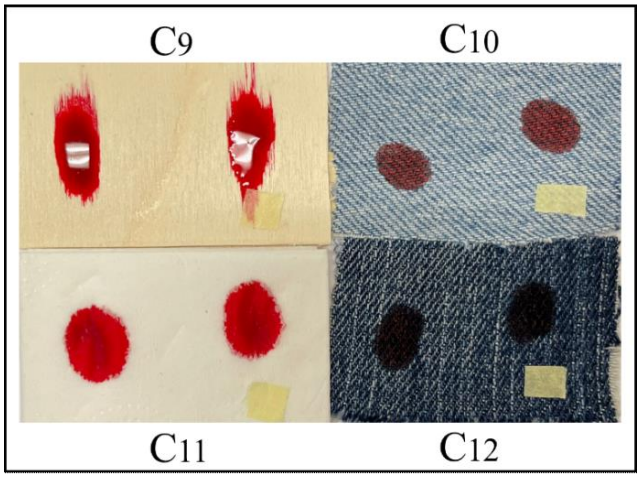

Figure 19: Drops of blood on inner and external margin of the samples.

5.2 Test bench

The test bench is composed of Hyperspectral camera and two halogen lamps as lighting system.

The model of the Hyperspectral system used to obtain our data is the HinaLea 4250. This model features a tunable filter positioned in front of the sensor to sequentially select the visible and near infrared spectral bands in a spectral range between 400 nm and 1000 nm (for a maximum of 300 spectral bands), with a step size of 2 nm [70]. The hyperspectral cube is then generated by collecting images for each spectral band-pass [70]. This camera presents high spatial resolution of 2.3 MP, and the scan angle is perpendicular to the object [70]. The camera includes a software called TruScope® Application Software 1.0.9, through which the images were acquired. TruScope® also allows to adjust the spectral range, perform calibration to compensate the acquired images, and auto-exposure to avoid saturated images [70]. TruScope® allows to recover the spectral information selecting the region of interest on the image by using several areas offered by itself, such as rectangle, ellipse and circle [70]. Reflectance spectrum of the region of interest obtained through this procedure is the mean of the reflectance spectra of all the pixels belonging to this area, and the mean is made by TruScope® itself. Hyperspectral camera and TruScope® Application Software 1.0.9 are shown in Figure 20 and Figure 21 respectively.

Figure 20: Hyperspectral camera: HinaLea 4250.

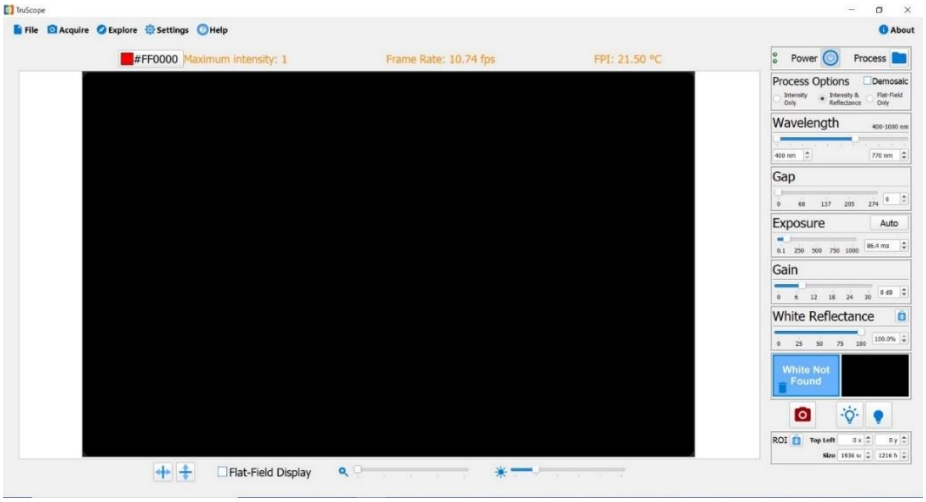

Figure 21: TruScope® Application Software 1.0.9.

The source of illumination is characterized by two halogen lamps symmetrically fixed on the hyperspectral camera so as to be perpendicular to the analyzed sample.

The schematic representation of the test bench is reported in the Figure 22.

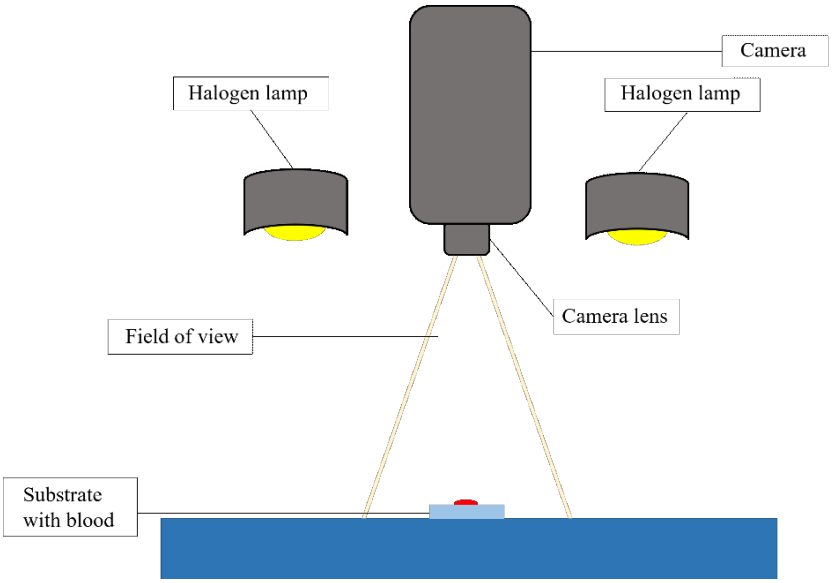

Figure 22: Schematic representation of the test bench.

5.3 Sample preparation

The samples consisting of a series of substrates on which one blood drop was deposited. Blood given by a healthy female volunteer, was collected in acid Vacutainer containers containing EDTA, an anticoagulant, and was placed with her consent on several types of substrates previously cleaned. The blood was deposited through the use of a pipette in order to obtain a constant size of the bloodstains of about one centimeter in diameter, and with a uniform amount of blood. The substrates used in this study are twelve, and they have been chosen because differ from each other not only in colors but also in textures. Different types of colors have been chosen because on light colored materials blood is visible to the naked eye, and these colors have little or no influence on the blood spectrum, while there are other materials whose colors affect the blood spectrum degrading it or blending with it, such as dark and red colors. The twelve samples were subdivided in three groups of four samples allowing the simultaneous acquisition of four samples, in order to reduce the number of acquisitions per day, and to avoid overheating of the camera itself. So four samples at a time were placed on a single support as shown in Figure 23, and each substrate is identified by an identifying name (ID) as shown in Table II.

Table II

Substrates	**ID**
Black paper	C_1
White paper	C_2
Yellow paper	C_3
Red paper	C_4
White tile	C_5
Green sponge	C_6
Red fabric	C_7
Cardboard	C_8
Wood	C_9
Light jeans	C_{10}
Napkin	C_{11}
Dark jeans	C_{12}

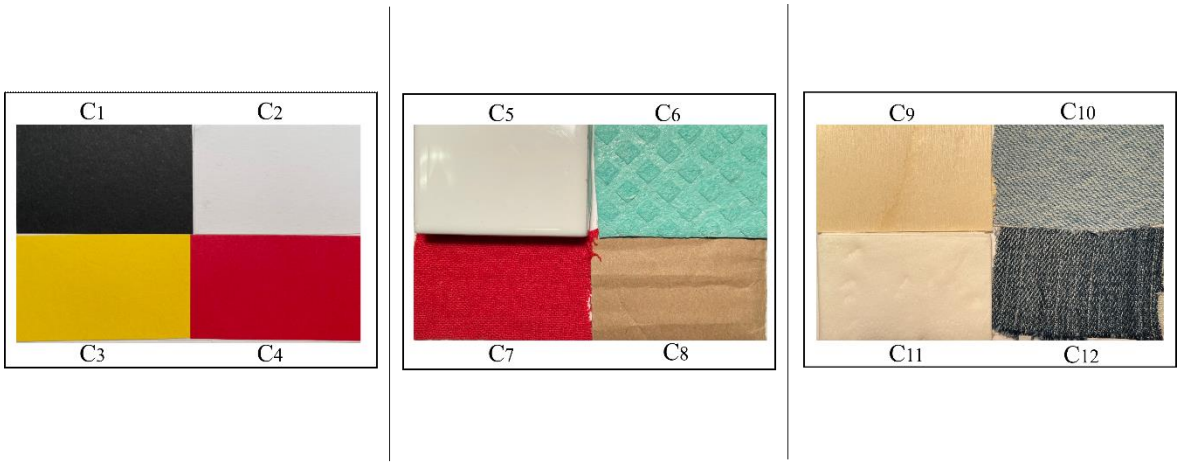

Figure 23: Samples.

The drop of the blood was placed close the inner margin of the sample as shown in Figure 24. The blood drops were deposited simultaneously on the four samples of the same single support, and the same was repeated for the other two supports, but with an interval time of five minutes between the depositions made on the different supports.

A reference sample was chosen between the twelve samples, and it is the white ceramic tile identified by C_5 .

Samples under examination were kept at constant laboratory temperature of 22 ± 2 degrees. Each sample is characterized by a length of 5.25 cm and an height of 3.25 cm.

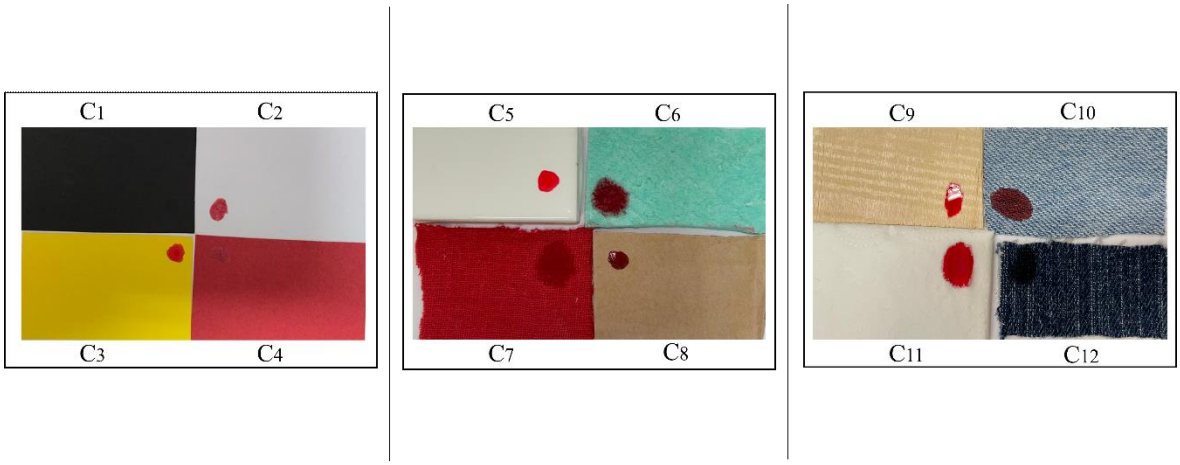

Figure 24: samples with bloodstains

5.4 Data collection

The spectral range considered for the acquisition of the images is between 400nm and 770nm with a step size of 2nm (185 nominal spectral bands), as this interval includes the spectral features of the blood.

Before acquiring the images the calibration procedure was performed for reflectance measurements. The calibration procedure, including the acquisitions of both dark reference and white reference, were performed to compensate the acquired images [13]. The dark and white references were acquired following the procedure on the user manual of the hyperspectral camera. Dark reference images were obtained by completely covering the lens chamber using the lens cap, and pressing the dark bulb icon on the user interface. While recording dark images, TruScope scans and saves images across all gain settings. White reference images were acquired with the use of a uniform reference white target shown in Figure 25.

In this study, the acquisition of dark reference was performed once before all acquisitions of the images, while the acquisition of white reference was performed before each single acquisition.

Figure 25: Uniform reference white target.

After the calibration procedure and so before the acquisition of the image, auto-exposure command was executed to correctly determine the amount of light reaching the sensor, so saturated images are avoided. In finally the image was acquired.

The time for setting the calibration, the exposure and image capture is about three minutes. The HIS cubes of the samples were captured for 14 days. During the first day an acquisition was made 30 minutes after blood deposition, and other acquisitions were carried out every hour for eight hours after blood deposition, in order to observe the dynamic spectral changes due to hemoglobin oxidation. While for the following days, the acquisitions were gradually reduced to one acquisition per day, in order to observe the spectral alterations due to blood aging.

Finally the hyperspectral data were pre-processed and analyzed using custom routines developed in MATLAB 2017 and Python.

5.5 Data analysis: data pre-processing and data processing via ANN

In the acquired image the bloodstain is the region of interest, and for each image the reflectance spectrum of each pixel belonging to the bloodstain was obtained by selecting manually the area belonging to the bloodstain. The area was selected manually through a code implemented in Python, which allows to select the region of interest for each image, ensuring that all the selected regions had the same area.

Every single pixel belonging to the blood drop, for all samples and all times, was treated as a single observation, and each observation was labeled according to the substrate and acquisition time. In finally, collected reflectance spectra were normalized with respect to the maximum reflectance value recorded in the reference substrate C_5 at time $t = 0h$.

The data obtained through the procedure explained previously were divided into three sets with a split ratio of 8:1:1: training, validation and testing. The first two datasets were used for the training and optimization of the model, while the third dataset was used to test the performance of the final model.

The neural network model proposed in this work for the background correction is the Multilayer Perceptron. MLP involves a regression that allows the prediction of real valued quantity, that are corrected reflectance spectra [58]. This model aims to predict new outputs given new statistically independent input data [58]. The network takes as input the reflectance spectra of bloodstain on a substrate C_n at time t_i, and outputs are the spectra of the bloodstain would have on a white reference substrate, C_5 at time t_i .

Data training provided to the network are as input data the reflectance spectra of pixels belonging to the bloodstain on a substrate C_n at time t_i, and as output data the reflectance spectra of pixels belonging to the bloodstain on a white reference substrate, C_5 at time t_i.
The neural network model used in this study is shown in Figure 26.

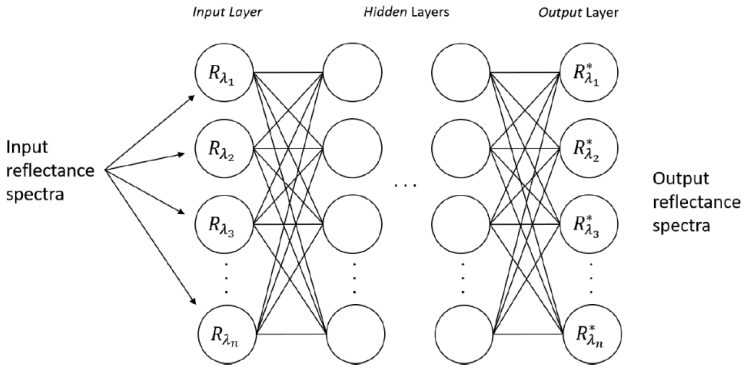

Figure 26: Multilayer Perceptron model. Figure taken and modified from [58].

As mentioned above, MLP is trained by means of the backpropagation algorithm, which is based on the backpropagation of the error value from the output layer through the neurons of the hidden layer, in order to adjust weights and bias of the network to reduce the error of the model iteratively. The loss function is the function that indicates the performance of the model, and through which the error value is calculated. MLP uses a stochastic gradient descent optimization algorithms to change the parameter of the model, to reduce the error and increase model performance. These concepts are explained in detail in the section 3.
The coefficient of determination R^2 is used as loss function.
The formula of the coefficient of determination R^2 is reported in the equation (7) [71].
In the numerator, λ_i is the observed dataset and λ_i^* are the predicted values, and both are used to calculate the *residual sum of squares*. In the denominator, $\bar{\lambda}$ is the average of the observed data, and is used for the calculation of the *total sum of squares* [71]. The value R^2 varies between - ∞ and 1 [71]. If this value is negative the model does not follow the trend of the data, while if it is 1 the model explains the data perfectly [71].

$$R^2 = 1 - \frac{\sum_{i=1}^{n} \lambda_i - \lambda_i^*}{\sum_{i=1}^{n} \lambda_i - \bar{\lambda}} \quad (7)$$

5.5.1 Bayesian optimization: hyper-parameters tuning

In this work the neural network model is generated through the Bayesian optimization approach, in fact the number of layers, neurons and hyper-parameters are tuned according to a Bayesian optimization approach [72]. Hyper-parameter optimization in machine learning aims to find the best hyperparameters of a machine learning algorithm, so that it returns the best performance given a validation set [72].

The hyper-parameters of a model, unlike the parameters that are learned by the model during the training period, are set by the machine learning engineer, and must be optimized in order to obtain better model performance [72]. This is done by giving to the model fit previously on training data the validation dataset, and the results will be used to update the hyper-parameters [72]. Hyper-parameter optimization aims to find a set of hyper-parameters that maximize a function [72]. However, the evaluation of a function to find the right set of hyper-parameters is complex, especially if the number of hyper-parameters is high [72]. The complexity is related to the fact that each time that different hyper-parameters are tested the model must be trained on the training data, predictions must be made on the validation data, and finally the function must be evaluated. Some approaches have been developed to overcome these problems [72]. The Bayesian optimization approach is advanced and fast in the optimization of hyper-parameters for neural networks, unlike the more classical methods such as randomized search and grid search [72].

The Bayesian optimization technique performs the training many times with different numbers of layers, neurons, and hyper-parameters. Initially, the function is tested n times by assigning casual values to its variables so as to diversify the exploration space. After this step, based on the results obtained, the Bayesian optimization begins. At each step the algorithm evaluates the past model information to select new optimal parameter values in order to increase the model performance. The first step is the definition of the function to be optimized. In this case, the objective function is constituted by the neural network model which takes as input several parameters, and as output the coefficient of determination R^2. The optimization aims to maximize this coefficient. The second step is to determine which input parameters of the objective function have to be optimized and also their corresponding bounds, as this is a constrained optimization method. The input parameters of the objective function that are made to vary in order to optimize R^2 coefficient are:

- Hyper-parameter *batch size (bs)*: it defines the number of sub-samples of the training data that will be propagated through the network. This hyper-parameter has been made to vary between 16 and 256 [73][74].
- Hyper-parameter *learning rate (lr)*: it defines how much to modify the model based on the estimated loss each time that the model weights are updated by the optimizer. This hyper-parameter has been made to vary between 0.0001 and 0.1 [73][74].
- Hyper-parameter *number of epochs (e)*: it defines the number of time that a whole dataset is propagated through the neural network. The number of epochs has been made to vary between 20 and 200 [73][74].
- Hyper-parameter *activation function (af)*: it takes in input the weighted sum of an artificial neuron and it defines how this sum is transformed in output. The activation function was chosen from linear, ReLU, Tanh, and Sigmoid [73][74].
- Hyper-parameter *normalization layer (n)*: it defines the presence or not of the batch normalization, which normalizes the values passed to it for each batch. Generally, the value of the normalization layer is 0 or 1, according to the presence of the normalization layer [73][74].
- *Number of hidden layers (nl)* have been made to vary between 1 and 12 [73][74].
- *Number of neurons per hidden layer (nn)* have been made to vary between 10 and 400 [73][74].

The defined objective function is shown in the equation (8).

$$R^2 = f(x, y, bs, lr, e, af, n, nl, nn) \quad (8)$$

where x is the input spectrum, and y is the output spectrum.

5.6 Statistical analysis

Several statistical tests have been conducted in order to make an experimental evaluation of this study. In detail, an analysis of the model accuracy on the reconstruction of the blood spectra corrected from the background influence was performed. The accuracy of the predicted spectrum was defined as the mean percentage error together with standard deviation, and with their behaviors as function of wavelengths, time and substrates.

In statistics, the *mean percentage error* (MPE) is the mean of the percentage error, in which the variation between the actual output of the network and the expected value is extracted in the form of percentage, and is called percentage error [75].

MPE is given by the difference between the predicted spectra resulting from the neural network model and the reference spectrum of the bloodstain on the white reference tile, averaging the reflectance spectra of all the pixels belonging to the bloodstain. The analysis has been done on samples of different materials and acquired at different times, so the mean percentage error will vary depending on the substrate, on the acquisition time, and on the wavelength range.

In statistics, the *standard deviation* measures the dispersion of a dataset relative to its mean, and is calculated as the square root of the *variance*, in which the variance measures how far each data in the set is from the mean and so from every other data in the set [76][77]. Standard deviation measures the absolute variability of a distribution, higher is the variability and greater is the standard deviation and greater will be the magnitude of the value deviation from the mean [78].

6 RESULTS

In this section, the spectra corrected from the background influence resulting as the outputs of the neural network, and the statistical analysis for the evaluation of the model accuracy will be reported.

The architecture of the neural network for the background correction was generated through the Bayesian optimization. After training and validation, the resulting model is composed by 5 hidden layers with 407, 201, 120, 78 and 11 hidden neurons respectively. The optimal activation function selected for the hidden neurons is ReLU function, while the optimal activation function selected for the neurons of the output layer is a linear function. The other hyperparameters that guarantee the highest R^2 value are the following:

- batch size (bs) = 128
- epochs (e) = 90
- learning rate (ls) = 0.0001
- normalization (n) = 0

Finally the model is tested and the results obtained are an R^2 value of 0.62 and a mean absolute error of 0.038.

In Figure 27 is reported the result obtained after the correction of the background made on the wood. In (a) are shown the reflectance spectra of the single pixel: reflectance spectrum of the blood on wood C_9 at time t=50h used as input for the model (blue), the corrected spectrum at t=50h given as output from the model (green), and the reference reflectance spectrum of the blood on white tile C_5 at time t=50h given as ground truth for the model (orange). In (b) are reported the same spectra, but obtained by averaging the predicted spectra of the pixels belonging to the bloodstains.

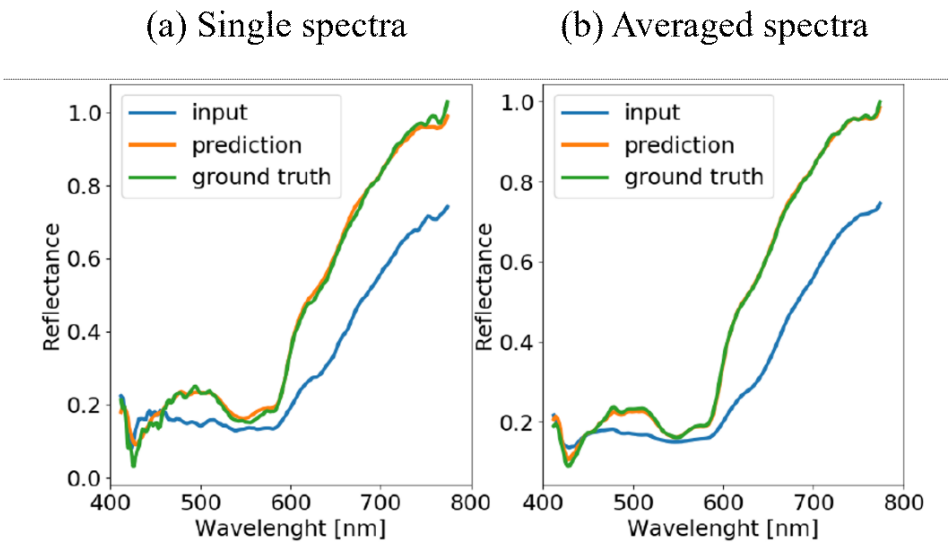

Figure 27: Neural network background correction on wood substrate at time t = 50h: comparison between blood reference spectrum (green), original blood spectrum on wood (blue), and correct predicted blood spectrum (orange); (a) blood spectra of single pixels, (b) average blood spectra.

In Figure 28 is shown the result obtained after the correction of the background, made on black paper. In (a) are shown the reflectance spectra of the single pixel: the reflectance spectrum of the blood on black paper C_1 at time t=50h used as input for the model (blue), the corrected spectrum at t=50h given as output from the model (green), and the reference reflectance spectrum of the blood on white tile C_5 at time t=50h given as ground truth for the model (orange). In (b) are reported the same spectra, but obtained by averaging the predicted spectra of the pixels belonging to the bloodstains.

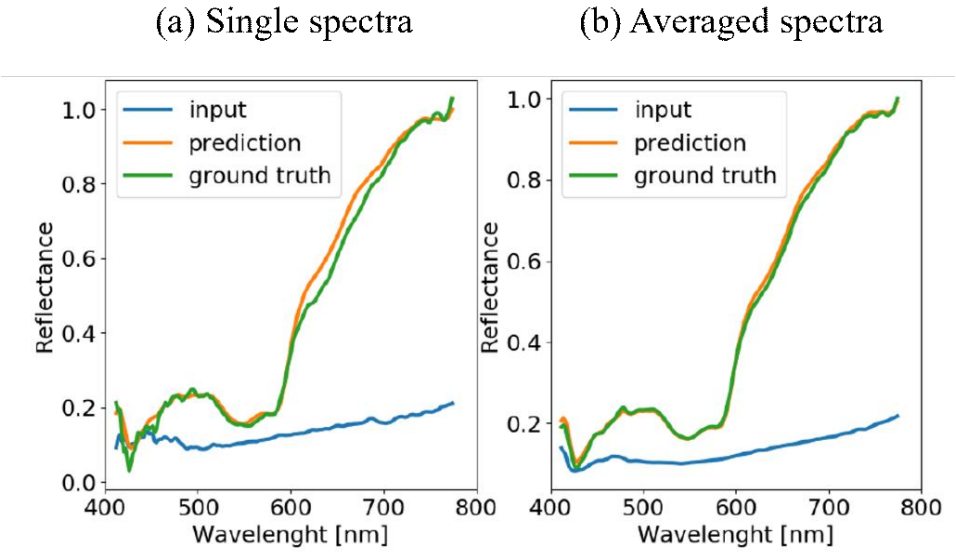

Figure 28: Neural network background correction on black paper substrate at time t = 50h: comparison between blood reference spectrum (green), original blood spectrum (blue), and correct predicted blood spectrum (orange); (a) blood spectra of single pixels, (b) average blood spectra.

The Figure 29 illustrates the statistical distribution of the mean percentage error.

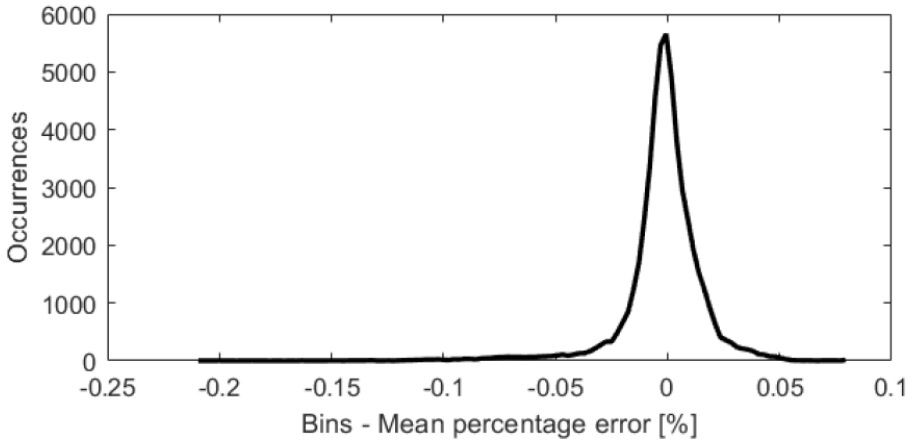

Figure 29: Statistical distribution of the mean percentage error, obtained by taking all the errors of all the samples examined, i.e. all the substates, all the acquisition times, and the entire spectral range considered.

The Figure 30 shows the mean percentage error and standard deviation in function of each wavelength, for all substrates and for all times.

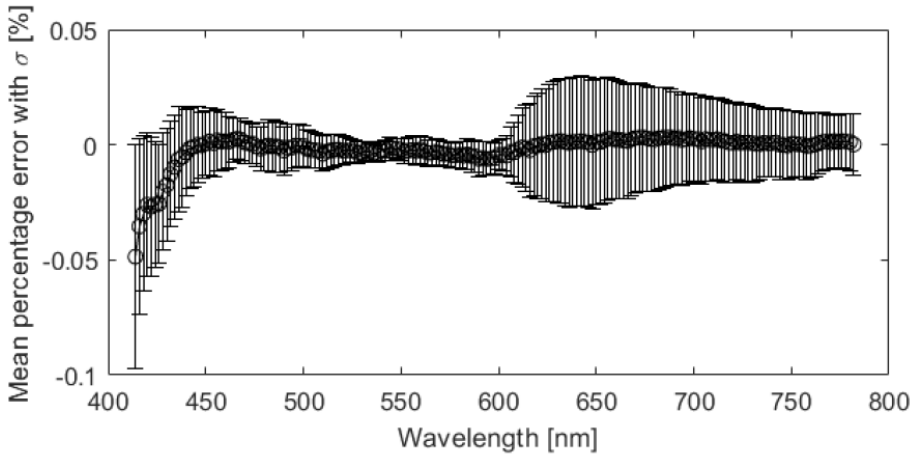

Figure 30: Mean percentage error and standard deviation in function of each wavelength, for all the substrates examined and for all the acquisition times.

In Figure 31 are reported the mean percentage error and standard deviation of each substrate in function of all wavelengths, in (a) and (b) respectively.

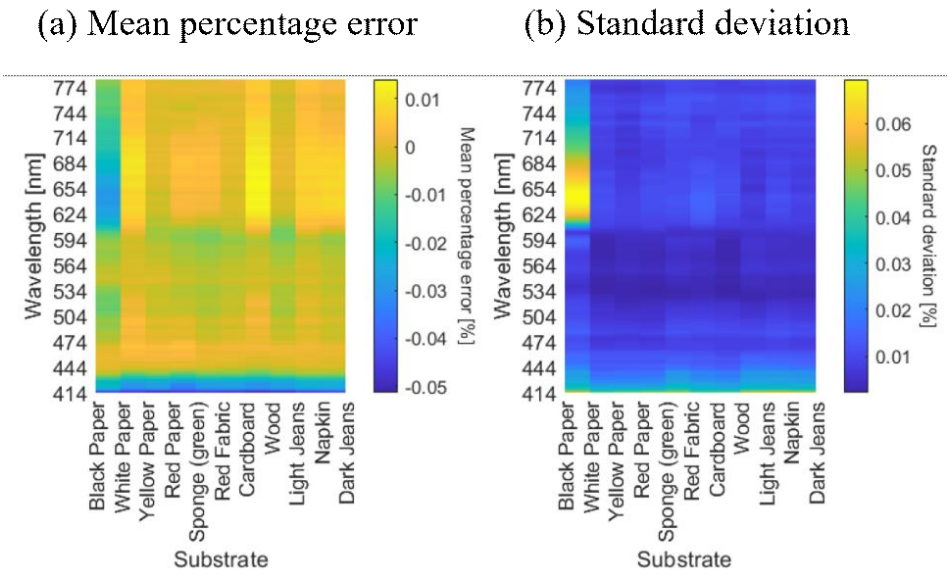

Figure 31: Mean percentage error (a) and standard deviation (b) of each substrate examined in function of the entire spectral range.

The mean percentage error and standard deviation of each substrates averaged within all the spectral wavelength are reported in Figure 32, in (a) and (b) respectively.

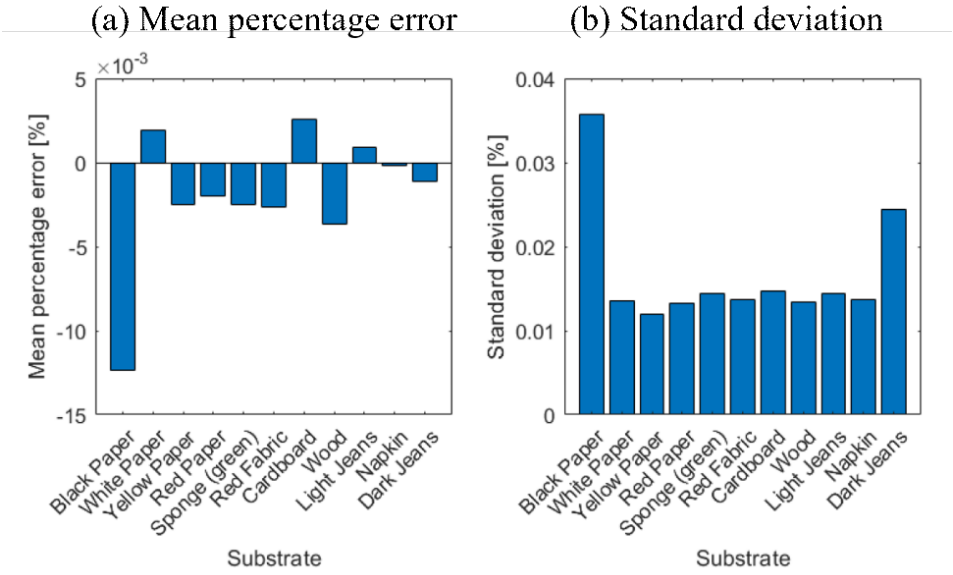

Figure 32: Mean percentage error (a) and standard deviation (b) of each substrate examined, averaged within the entire spectral range.

7 DISCUSSION

This work aims to remove the substrate contribution in the reflectance spectrum of the blood drop deposited on this substrate, by using the neural network. However, before doing this it was necessary to obtain the optimal data (reflectance spectra) to be supplied to the network.

The first step was the definition of the test bench to obtain optimal data to be analyzed, and the preparation of the sample to optimize the acquisitions of a large number of samples, for this reasons three preliminary tests were performed. The first preliminary test together with the second helps to define the test bench, but also gives information on the preparation of the sample, while the third preliminary test aims to optimize sample preparation.

The part of the work relating to the definition of the test bench and sample preparation was carried out in collaboration with Delia Iafelice, for her thesis entitled "*Hyperspectral imaging in forensic science: definition of the test bench and age estimation of bloodstains on different substrates*".

The blood given by a healthy female volunteer, was collected in acid Vacutainer containers containing EDTA, an anticoagulant. The use of an anticoagulant was necessary to avoid blood clotting. In fact, this made it possible to perform more precise depositions, at the predetermined times, avoiding blood clotting over time.

In the test bench the illumination system is extremely important as it must be able to guarantee optimal spectral data corrupted by little noise, but at the same time it does not interfere with the chemical processes occurring in the blood. In this study, was decided to use halogen lamps as illumination system because they are easy to find, and guarantee a quite uniform and broadband illumination [13].

However, halogen lamps reach very high temperature causing the objects to catch fire [80]. For this reason it has been necessary to understand how many lamps to use.

The first two preliminary tests were performed with the aim of determining how many halogen lamps to use in order not to damage the samples examined. During the first preliminary test were used four halogen lamps as illumination system. The problem was that the heat accelerated the aging process of the blood. In particular, the strong heat has "cooked" the blood over the substrate which immediately dried up and changed color, indicative of the fast aging process. Moreover, the number of substrate used was so high,

23 samples, that it did not allow precise acquisitions at the predetermined times, and the deposition of the blood drops on all the substrates at the same time before the beginning of the acquisitions, contributed to accelerate the aging process of some sample, since the last sample was acquired after the required time to acquire 22 samples. For this reasons the first test was interrupted to perform a second test with a reduced number of samples and lamps.

The second preliminary test was performed with 15 samples and two halogen lamps. The blood was deposited on the samples with an interval time of 5 minutes (time required for one acquisition), in order to avoid the problem previously explained. In this case the use of two lamps did not affect the aging process of the blood, as the heat generated was reduced. However this test was interrupted for another problem related to the environmental light turned on (fluorescent lamps), in fact this light influenced the blood spectra at wavelength of 542 nm. Remember that the β peak of the blood spectrum is at ~542 nm, and its behavior over time is useful for estimating the age of blood. Over time this peak should decrease, however with ambient lights on the peak exhibits a high prominence. The cause of this high prominence is the fluorescent light on that present two main emission lines, one at approximately 544 nm and the other one at 611 nm [81]. Moreover, fluorescent lamps spectra are characterized by sharp emission lines and present a high variability spectrum [81]. Consequently to avoid this problem the ambient lights must to be turned off. This second test confirmed the use of two halogen lamps as illumination system, but at the same time showed a limitation of the hyperspectral camera in a real forensic application, since the acquisitions must not be made in the presence of other lighting sources besides the one chosen.

The third preliminary test was performed with the aim of finding the optimal region where to deposit the blood drop over four samples placed on the same support. The previous two test have been performed acquiring individually the samples, and the sample was placed approximately in the center of the field of view of the camera. However, the high number of samples and the individually acquisitions generated complexity during the acquisitions, as well as being time consuming. To overcome this problem the number of samples was further reduced from 15 to 12, and to optimize the acquisitions it was decided to place 4 samples on the same support with a size of each sample of 5.25cm * 3.25cm. The samples were cropped like this because in order to cover the field of view of the camera. In this way the time required for the acquisitions was reduced, and furthermore the pre-

established acquisition times were respected. The only problem was to decide where placed the drops of blood over the 4 samples. Two drops of blood were deposited: one over the inner margin of the sample and one over the external margin of the sample. This test was performed only on four samples (Wood, Light Jeans, Napkin, Dark Jeans) over a single support; there was no a specific reason for which these substrates were chosen. The results are reported in the Figures 33, 34, 35, 36, in which is possible to see a comparison of the absorbance spectra of the two blood drops placed in two different areas of the substrate. The absorbance spectra of the blood placed on the inner margin of the substrate are affected by less noise with respect the blood placed on the external margin of the substrate. In particular, the absorbance spectra of the blood drop on inner margin shows always the Soret peak because the low wavelength are affected by less noise, and the peaks α and β are more visible especially for the Dark Jeans and the Wood. This behavior can be explained considering that the blood drops on the inner margin of the substrates are exactly under the camera lens, so are affected by less noise and distortion.

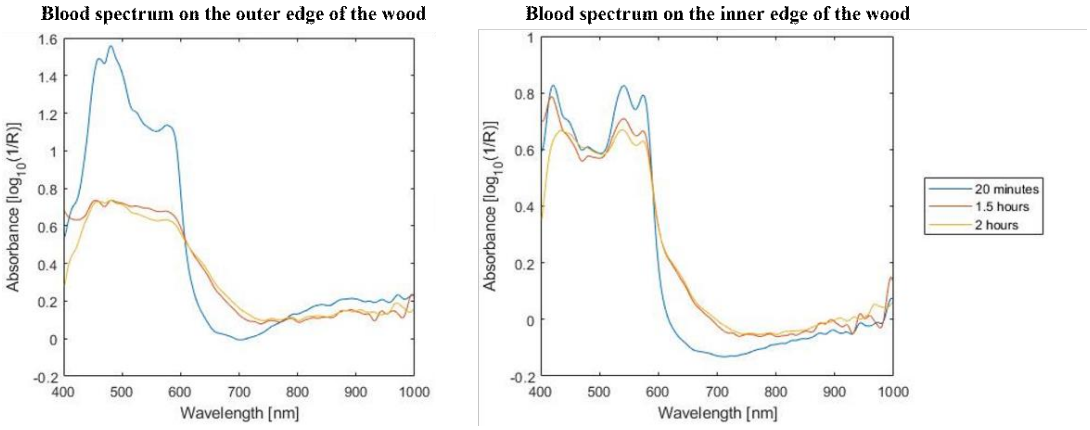

Figure 33: Right: Absorbance blood spectra of bloodstains on the outer edge of the wood at different times: 20 minutes (blue), 1.5 hour (red), 2 hours (orange). Left: Absorbance blood spectra of bloodstains on the inner edge of the wood at different times: 20 minutes (blue), 1.5 hour (red), 2 hours (orange).

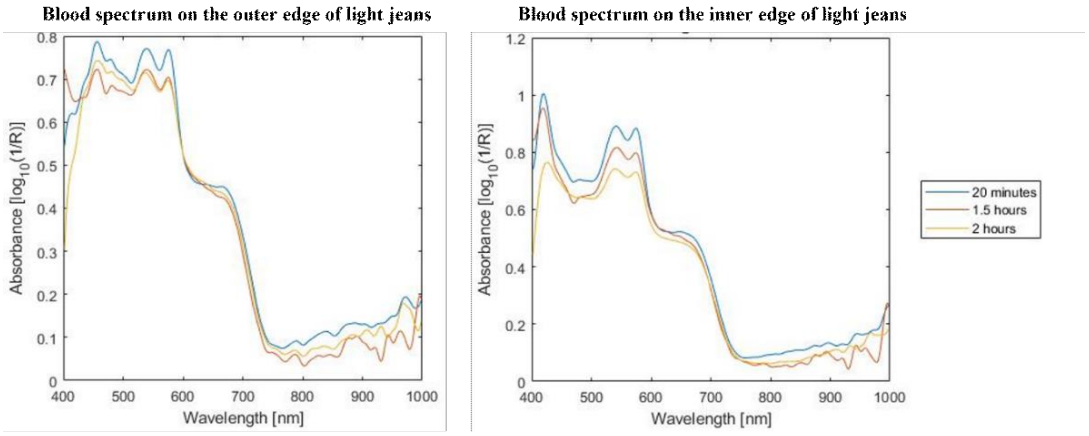

Figure 34: Right: Absorbance blood spectra of bloodstains on the outer edge of light jeans at different times: 20 minutes (blue), 1.5 hour (red), 2 hours (orange). Left: Absorbance blood spectra of bloodstains on the inner edge of light jeans at different times: 20 minutes (blue), 1.5 hour (red), 2 hours (orange).

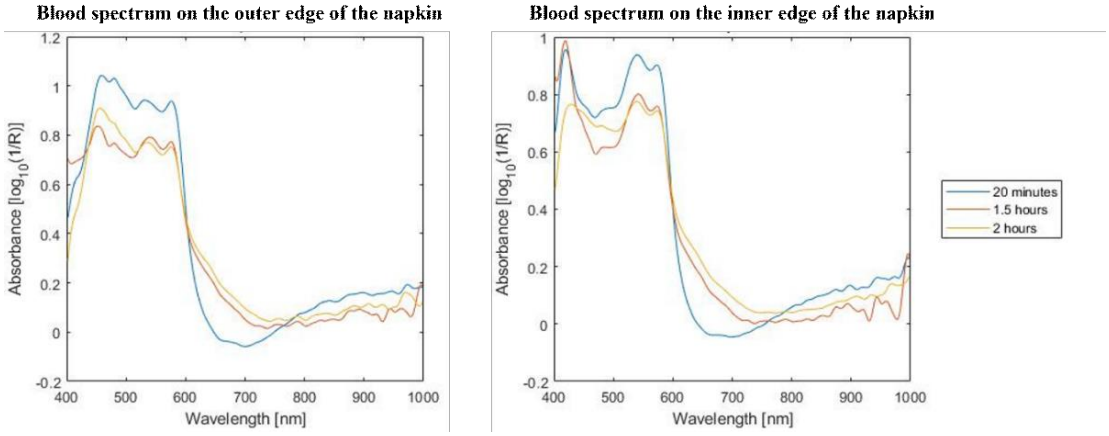

Figure 35: Right: Absorbance blood spectra of bloodstains on the outer edge of napkin at different times: 20 minutes (blue), 1.5 hour (red), 2 hours (orange). Left: Absorbance blood spectra of bloodstains on the inner edge of napkin at different times: 20 minutes (blue), 1.5 hour (red), 2 hours (orange).

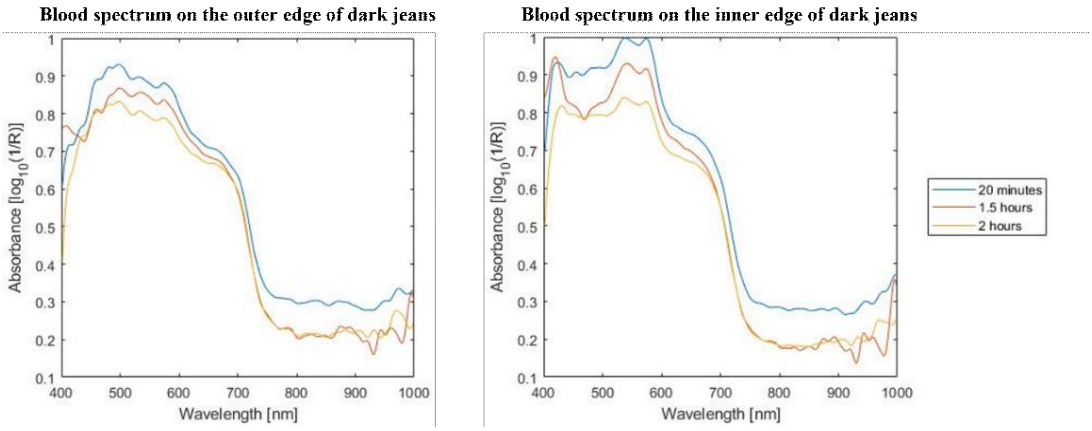

Figure 36: Right: Absorbance blood spectra of bloodstains on the outer edge of dark jeans at different times: 20 minutes (blue), 1.5 hour (red), 2 hours (orange). Left: Absorbance blood spectra of bloodstains on the inner edge of dark jeans at different times: 20 minutes (blue), 1.5 hour (red), 2 hours (orange).

The last thing decided during this test was how to perform the calibration. In the first two tests the white and dark calibration was performed before the beginning of the acquisitions. In this case, it has been decided to maintain the dark calibration before the beginning of the acquisitions, but to perform the white calibration before each acquisition, to compensate the errors that could arise from the calibration of the sensor, and to reduce thermal noise cause by the prolonged used of the camera [82][83]. Instrumental error and thermal error cause noise on the spectral bands, and reducing the efficiency of the Hyperspectral system in performing analysis [83].

After performing preliminary tests the optimal test bench was defined to derive optimal data to use in the neural network. In addition, these tests show how to prepare the samples before the acquisitions, and how the calibration procedure should be performed. The test bench consists of:

- Hyperspectral Camera, HinaLea 4250 model.
- Two halogen lamps symmetrically placed on the camera as to be perpendicular to the sample examined.
- Environmental light (fluorescent lamps) switched off.

The 12 chosen samples were organized in three groups to optimize the acquisitions of a high number of samples, reducing the time required for acquisitions and respecting the pre-established acquisition times. Four samples were placed on a single support, in order to

obtain three supports, and the blood drop was deposited on the inner margin of each sample, with an interval time of 5 minutes between the substrates of one support and the other one. In addition, the calibration procedure for reflectance measurements is characterized by performing the dark calibration performed once before the start of all acquisitions and performing white calibration before each acquisition. Finally, for the data collection it was decided to acquire only the spectral range from 400nm to 770nm as this range includes the spectral characteristics of the blood. Furthermore, in this way the acquisition times are faster than the acquisitions made on the entire spectral range offered by the camera that goes from 400nm to100nm.

Once the test bench was defined, the hyperspectral cubes of all twelve samples were acquired, and the reflectance spectra were achieved.

The problem is that the substrates affect the aspect of the blood and its spectrum, degrading it or blending with it. In detail, a substrate influences the blood spectrum because a colored background absorbs visible light disturbing the measured reflectance spectra of the bloodstains [15]. For this reason it is useful to remove the contribution of substrates in the reflectance spectra of the bloodstains, obtaining correct reflectance spectra, before proceeding with other analyzes, and this is done with the use of a neural network.

The neural network model exploited for the background correction is the Multi-Layer Perceptron optimized through Bayesian optimization approach. The neural network was developed by the research group of the department where I did the internship, and then adapted to this work.

The Multi-Layer Perceptron was chosen because involves a regression that allows the prediction of real valued quantity, that are corrected reflectance spectra [58]. The network is trained by the backpropagation algorithm, a supervised learning algorithm, which function is to adjust the weights and bias of the network through the backpropagation of the error value, that is obtained by a loss function, and in this way reduces the error iteratively [64]. Therefore the loss function indicates the performance of the model, and the coefficient of determination R^2 has been chosen as loss function, because this is a regression model and because it provides more information with respect than SMAPE, MAPE, RMSE and MAE in regression analysis evaluation [84].

The architecture of the Multi-Layer Perceptron was generated through the Bayesian optimization, which aims to maximizes the loss function to obtain the best model

parameters. Bayesian optimization was chosen to automatically optimize the number of hidden layers, hidden neurons and other hyperparameters, instead of being manually optimized by a machine learning engineer [72]. This optimization approach was chosen because is advanced and fast in the optimization of hyper-parameters for neural networks, unlike the more classical methods, such as randomized search and grid search [72]. The objective function chosen is constituted by the neural network model, which takes as input several parameters, and as output the coefficient of determination R^2. The optimization consists in varying these parameters in order to maximize this coefficient, because the value R^2 varies between - ∞ and 1, and if this value is negative the model does not follow the trend of the data, while if it is 1 the model explains the data perfectly [71].

The goal is to use the network that takes as input the reflectance spectra of bloodstain on a substrate C_n at time t_i, and outputs are the spectra that the bloodstain would have on a white reference substrate, C_5 at time t_i . White ceramic tile C_5 was chosen as reference for two main reasons:

- the white color does not absorbs at any wavelength, so does not affect the spectral features of the bloodstain spectrum, ensuring its proper visualization, without the interference from the substrate color [15].
- the tile is a non-absorbent material makes it possible to have no distinction between the reaction that the blood may have on the substrate surface and on the substrate portion where it is absorbed [85].

Since a neural network needs a training period, during which it sees and learns from labeled examples what features are required to obtain a desired output given a certain input, training data has been defined to train the network. In addition, validation data used to optimize the hyperparameters of the network, and testing data to test the final network has been defined.

Initially it was thought to use the reflectance spectra of the bloodstains as data. However, the number of bloodstains on samples (11 substrates) is too low to train a network. The network requires a high number of training data (input data and output data) for its training, in fact the more labeled examples are provided to the network, the better its performance will be [51].

Since Hyperspectral imaging system is a reflectance spectroscopy technique, that provides the possibility of obtaining a reflectance spectrum for each pixel of the acquired image, it

was decided to treat every single pixel belonging to the bloodstain, for all samples and all times, as single observation; each observation was labeled according to the substrate and acquisition time. In particular, it was decided to provide the network with the reflectance spectrum of each pixel belonging to the bloodstain of the substrate (region of interest), and not the reflectance spectrum of the entire bloodstain of the substrate, obtained by averaging the reflectance spectra of its pixel. In this way a large population of input data and output data was obtained, to train the network in a good way.

For this reason during the train the network takes as input data the reflectance spectrum of each pixel belonging to the bloodstain on a substrate C_n at time t_i, and as output data the reflectance spectrum of each pixel belonging to the bloodstain on a white reference substrate, C_5 at time t_i.

In the acquired image the bloodstain is the region of interest, and for each image the reflectance spectra of the pixels belonging to the bloodstain was obtained by selecting manually the area belonging to the bloodstain. However, although the deposit of the blood drop on every substrate was performed with great precision, the size of the bloodstain varies according to the absorption of the blood on the different substrates. Consequently, the amount of pixel size for each drop is different. For this reason the area was selected manually through a code implemented in Python, which allows to select the region of interest for each image, making sure that all selected regions have the same area, and so the same number of pixels. In finally, collected reflectance spectra were normalized with respect to the maximum reflectance value recorded in the reference substrate C_5 at time $t = 0h$. The reflectance spectra of every pixel belonging to the bloodstain, for all samples and all time, were used not only for the train, but also for the validation and test of the network. In fact the data were divided into three sets: training, validation and testing with a slit ratio of 8:1:1. The first two datasets were used for the training and optimization of the model, while the third dataset was used to test the performance of the final model.

Once that the predicted spectra (corrected spectra) have been achieved as outputs of the neural network, they were analyzed through custom routines developed in MATLAB 2017. Before discussing these results different spectra will be shown before correction to demonstrate the need to remove the substrate contribution. Remember that in a reflectance spectrum the downward deflections indicate the wavelength ranges for which the material absorbs the incident energy, and these deflections are called absorption bands [38].

In Figure 37 is possible to see the reflectance spectrum of the bloodstain on white tile, and is evident the reason why it has been chosen as reference spectrum.

This spectrum shows the typical absorption peak of the blood according the literature. First of all the reflectance spectrum of the fresh blood in the visible region is dominated by the oxy-hemoglobin spectrum, because outside the body the hemoglobin exists as oxyhemoglobin [69].

It is visible the strongest peak called *Soret* peak at 415nm due to hemoglobin, and two weaker peaks, β peak at 542nm and α peak at 572nm, due to HbO_2 according to literature [7]. The red color of the blood is due to Soret peak, because this absorbs in the blue region of the visible spectrum between 400nm and 500nm, and reflects in the red region of the visible spectrum [68]. Furthermore, is present the steepness of the curve between 600nm and 650nm [5].

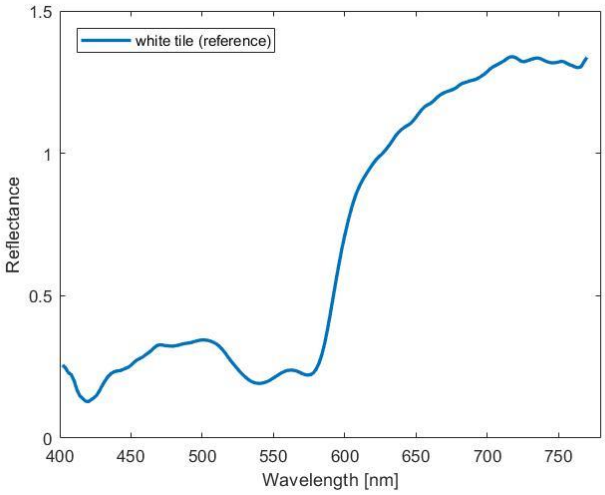

Figure 37: Reflectance blood spectrum on white tile (reference spectrum).

The Figure 38 shows the comparison between the reflectance spectra of the bloodstains on different substrates at time t = 0.5h and the blood reference spectrum at time t = 0.5h.

Materials of different colors have been chosen because on light colored materials blood is visible to the naked eye, and these colors have little or no influence on the blood spectrum, while there are other materials whose colors affect the blood spectrum degrading it or blending with it, such as dark and red colors.

Each reflectance spectrum shown in this figure is obtained by averaging all the reflectance spectrum of the pixels belonging to the bloodstain of the substrate C_n at same time t_i.

By comparing the blood spectra on various substrate, such as red paper, light jeans, dark jeans, with the blood reference spectrum (on white tile), is possible to see the influence of various substrates on the blood spectrum, and it is clear why it is necessary to remove its contribution. In fact, the blood reflectance spectrum on red paper (blue) does not present the two β and α peaks, while the blood reflectance spectrum on dark jeans (green) shows flat trend making it very difficult to discriminate the spectral features of the blood. The blood reflectance spectrum light jeans (orange) does not present the typical steepness of the fresh blood between 600nm and 650nm.

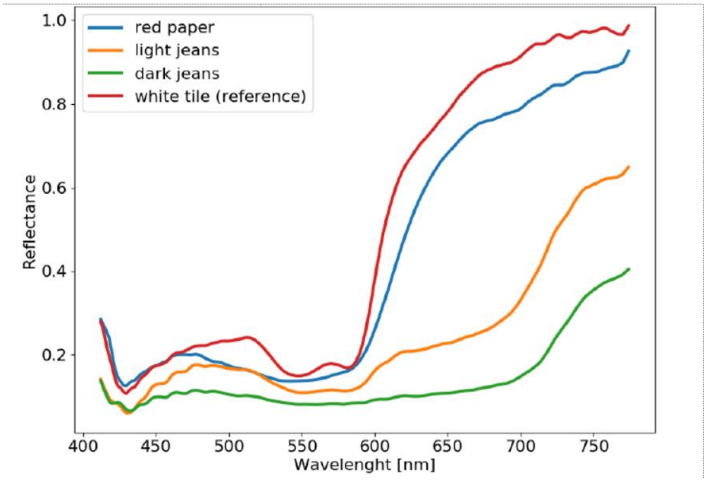

Figure 38: Comparison between blood reflectance spectra on different substrates at time t = 0.5h: blood reference spectrum (red), blood reflectance spectrum on red paper (blue), blood reflectance spectrum on light jeans (orange), blood reflectance spectrum on dark jeans (green) .

The Figures 39, 40, 41, allow to see how different substrates influence the trend of the blood spectrum, remembering that a colored background absorbs visible light disturbing the measured reflectance spectra of the bloodstains. Each reflectance spectrum shown in this figure is obtained averaging all the reflectance spectrum of the pixels belonging to the bloodstain of the substrate C_n at same time t_i.

The Figure 39 illustrates the comparison between the blood reflectance spectrum on red paper C_4 at time t = 0.5h (red) and the substrate itself (blue). The influence of the red paper on the blood spectrum is visible. In fact the red paper absorbs in the wavelength range in which β and α peaks of the blood spectrum are present, consequently these two peaks disappear from the blood spectrum. The trend of the blood spectrum is like that of the red paper, i.e. it is flat in the wavelength range in which the red paper absorbs.

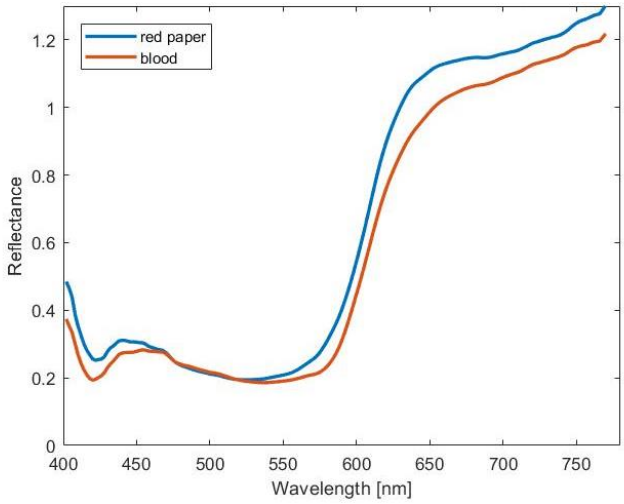

Figure 39: Comparison between red paper reflectance spectrum (blue) and blood reflectance spectrum of blood drop deposited on this substrate (red), at time t = 0.5h.

The same occurs for the dark jeans shown in Figure 40. This figure illustrates the comparison between the blood reflectance spectrum on dark jeans C_{12} at time t = 0.5h (red) and the substrate itself (blue). The influence of dark jeans on the blood spectrum is visible, in fact the blood does not have its spectral features. Dark jeans has a color close to black, and tends to absorb at almost all wavelengths. Consequently the blood spectrum tends to be influenced at almost all wavelengths, and therefore its trend is like that of dark jeans.

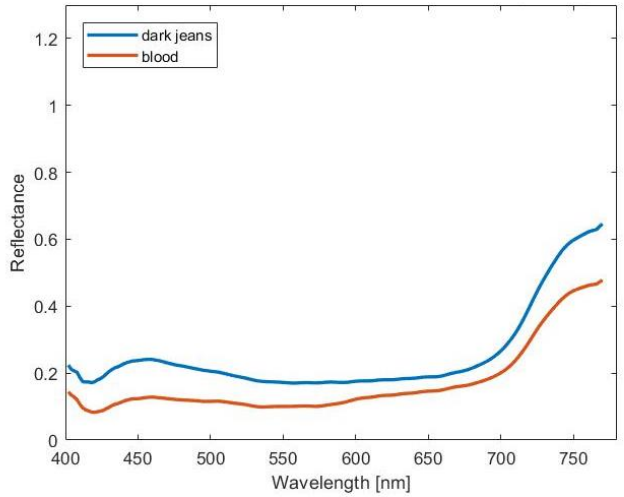

Figure 40: Comparison between dark jeans reflectance spectrum (blue) and blood reflectance spectrum of blood drop deposited on this substrate (red), at time t = 0.5h.

In finally in Figure 41 is shown the comparison between the blood reflectance spectrum on light jeans C_{10} at time t = 0.5h (red) and the substrate itself (blue). In this case the light jeans spectrum has an absorption band that involve the wavelengths from 600nm onwards. The consequence is that blood spectrum is influenced in this region, where the peak at 626nm due to the methemoglobin is found, causing problems in estimating blood age, as this peak grows over time [7]. For these reasons it is necessary to remove the contribution of the substrates, especially for those materials that degrade the blood spectrum, like dark materials, and for those materials that are confused with the blood spectrum, such as red materials.

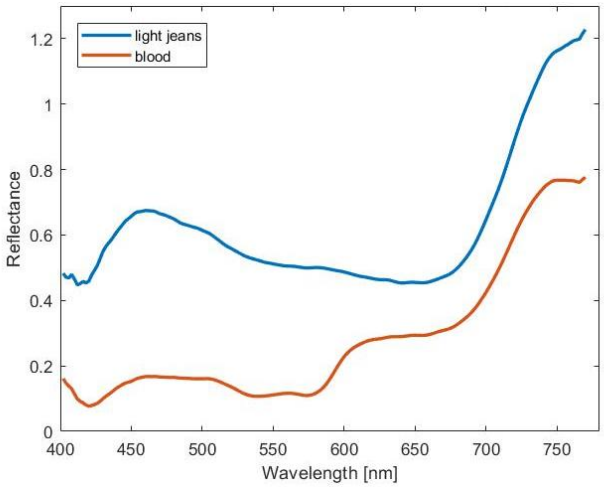

Figure 41: Comparison between light jeans reflectance spectrum (blue) and blood reflectance spectrum of blood drop deposited on this substrate (red), at time t = 0.5h.

In the following figures will be reported the results obtained by the network and the statistical analysis for the evaluation of the model accuracy.

The Figure 27 is reported the background correction on wood C_9 at time t = 50h. In (a) is shown the reflectance spectrum of the blood on wood C_9 at time t=50h used as input for the model (blue), the corrected spectrum at t=50h given as output from the model (green), and the reference reflectance spectrum of the blood on white tile C_5 at time t=50h given as *ground truth* for the model (orange). The reflectance spectra considered are of a single pixel. In (b) are compared the same spectra, but obtained by averaging the reflectance spectra of the pixels belonging to the bloodstains. First of all in both figures it is possible to see a clear change between the original spectrum and the predicted one. On the non-

corrected spectrum it is difficult to distinguish the typical peaks of the blood spectrum due to the influence of the substrate, therefore it will be difficult to try to recognize it. The use of the network allowed to remove the contribution of the substrate, and the result obtained is a predicted spectrum comparable with the white reference spectrum. The corrected spectrum now is clear, in fact has all the typical features of the blood spectrum, therefore it can be analyzed without problems. Furthermore, from the comparison between the single predicted spectrum and the averaged predicted spectrum, obtained by averaging all predicted spectra of the pixels belonging to the bloodstain, is possible to see that the averaged predicted spectrum almost overlaps the ground truth. This can be explained by considering that the spatial averaging removes the non-homogenous texture of the wood, so the variability of the pixels, which is a characteristic of typical materials considered in forensics. However, for more homogeneous materials such as black paper, the average does not result in substantial improvements in the prediction, as can be seen in Figure 28.

In Figure 28 is shown the background correction on black paper C_1 at time t = 50h. This color is very difficult to treat as mentioned above, but with the use of the neural network great results have been obtained. In fact, the contribution of the substrate is removed, and the corrected spectra shows the typical features of the blood spectrum. In this case the averaged predicted spectrum does not result in substantial improvements being a more homogenous material. The main deviation of averaged predicted spectrum from the ground truth is in the wavelength range between 600nm and 700nm.

In the following figures are reported the statistical results for the evaluation of the model accuracy.

The Figure 29 illustrates the statistical distribution of the mean percentage error, considering the errors of all samples examined, i.e. all the substrates, all the acquisition times, and the entire spectral range considered, between 400nm and 780nm.

The percentage error is given by the difference between the output obtained from the network (predicted spectrum) and the desired output (blood reference spectrum), expressed as a percentage with respect the value itself. The distribution of the mean percentage error is a zero-centered, almost Gaussian, with standard deviation $\sigma = \pm 0.05\%$. Obviously it can be noted that both the mean percentage error value and the standard deviation value are very low.

The Figure 30 allows to better understand what happens to each single wavelength. This figure shows the mean percentage error and standard deviation in function of each wavelength, for all substrates and for all acquisition times. The mean percentage error is the central curve represented by the circles, while the standard deviation is represented by the vertical bars. According the vertical bars at low wavelength, from 400nm to about 450nm, an increase in the standard deviation occurs. In this spectral range the halogen lamps used as illumination system does not guarantee a sufficient spectral intensity, causing problems in the measured reflectance blood spectrum and increasing the level noise at these wavelengths. In fact this lamp provides a better contribution for the high wavelength than the low wavelength, as shown in figure 42. For this reason the spectral interval between 400nm and 450nm is characterized by high level of noise, and a large standard deviation with respect the other wavelengths. After this spectral interval the uncertainty band became more stable above 450nm, up to 600nm, where there is an increase in the standard deviation in the wavelength range between 600nm and 650nm. The increase of the standard deviation in this spectral range is due to dark-colored substrates which by absorbing in these wavelengths cause greater uncertainty. This deduction is evident in Figure 31.

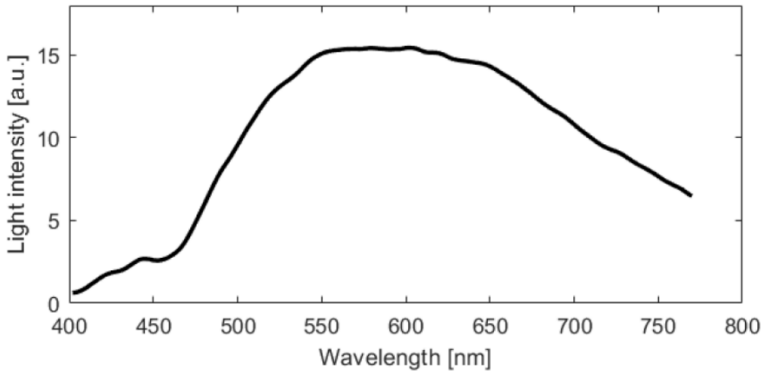

Figure 42: Intensity spectrum of the halogen lamp.

The Figure 31 shows the mean percentage error and the related standard deviation of each substrate for all spectral wavelengths, (a) and (b) respectively. As is possible to see this graphs confirm the increase of the standard deviation at the shortest wavelengths, and in the spectral interval between 600nm and 650nm only for the black paper. The black paper

can be the outlier that increases the standard deviation of all the samples as shown in Figure 30.

The mean percentage error and standard deviation of each substrates averaged within all the spectral wavelengths are reported in Figure 32, (a) and (b) respectively. This figure confirm the results reported in the previous one. Standard deviation is high in dark-colored materials, i.e. black paper and dark jeans. However the mean percentage error of the dark jeans is lower than the mean percentage error of the other substrates. This is due to the particular texture of this substrate that presents an high variability in its pixels, and when they are averaged the mean value decreased.

8 CONCLUSION

In this study Hyperspectral imaging system is used to perform a series of acquisitions of several substrate on which are present bloodstains. Hyperspectral imaging is a *reflection spectroscopy technique*, and consequently provides information on the *reflectance spectrum* for each point of the sample examined.

Through the spectral features of reflectance spectra of the bloodstains, i.e. Soret peak, α and β peaks, is able to identify the blood, and so to distinguish the blood from other substances that are similar in appearance and color. Once the blood is identified, it could be used for DNA analysis, and then to find out who is the suspect or victim of a possible crime scene. Furthermore, blood spectra can be used for estimating the age of blood, by observing the behavior of the blood spectral features over time. However, prior to do this analysis is necessary to obtain a reflectance spectra of the bloodstains clear, without the influence of the substrate on which they are deposited. In fact the substrates affect the blood spectrum, because a colored background absorbs visible light disturbing the measured reflectance spectra of the bloodstains. This thesis work presents a method to remove the contribution of a substrate in the reflectance spectrum of the blood drop deposited on any kind of substrate, by using Machine Learning method. Starting from reflectance spectra of bloodstains on different substrates, it is possible to obtain the reflectance spectra that the same bloodstains at the same time would have on a standard reference substrate, with a mean percentage error of 0.1% and a standard deviation of ±0.05%. The best reference substrate is a white substrate, because this color does not absorbs at any wavelength, so it does not affect the spectral features of the blood spectrum, ensuring its correct visualization without the interferences from the substrate color. For this study, materials of different colors have been chosen, because they cause more problems with respect the light colored materials, as they affect the blood spectrum degrading it or blending with it, such as dark and red colors.

The corrected spectra are achieved through the use of the Multilayer Perceptron, whose architecture and hyperparameters are obtained through the Bayesian optimization approach. This new approach enables high performance background correction for all tested substrates, being able to reduce the reflectance spectra of blood on different substrates to a reference blood reflectance spectrum.

The inaccuracy of the model is related to the black paper which being a perfect absorber is the color that gives more problems, and to the illumination source consisting of halogen lamps with an insufficient spectral intensity at shortest wavelengths. Hence, the use of lighting systems capable of covering a wider spectral range, towards the ultraviolet band, could strongly contribute to reducing the standard deviation at low wavelengths.

REFERENCES

[1] Siegel, Jay A.. "forensic science". Encyclopedia Britannica, 1 Jun. 2020, https://www.britannica.com/science/forensic-science. Accessed 4 February 2022.

[2] Dictionary of Forensic Science - Oxford Reference

[3] Definition of Forensic Science (all-about-forensic-science.com)

[4] What is Forensic Science? - Definition, History & Types - Video & Lesson Transcript | Study.com

[5] M. Zulfiqar, M. Ahmad, A. Sohaib, M. Mazzara, and S. Distefano, "Hyperspectral imaging for bloodstain identification," *Sensors*, vol. 21, no. 9, pp. 1–20, 2021, doi: 10.3390/s21093045.

[6] A. Majda, R. Wietecha-Posłuszny, A. Mendys, A. Wójtowicz, and B. Łydżba-Kopczyńska, "Hyperspectral imaging and multivariate analysis in the dried blood spots investigations," *Appl. Phys. A Mater. Sci. Process.*, vol. 124, no. 4, pp. 1–8, 2018, doi: 10.1007/s00339-018-1739-6.

[7] T. Bergmann, F. Heinke, and D. Labudde, "Towards substrate-independent age estimation of blood stains based on dimensionality reduction and k-nearest neighbor classification of absorbance spectroscopic data," *Forensic Sci. Int.*, vol. 278, pp. 1–8, 2017, doi: 10.1016/j.forsciint.2017.05.023.

[8] G. Edelman, T. G. van Leeuwen, and M. C. G. Aalders, "Hyperspectral imaging for the age estimation of blood stains at the crime scene," *Forensic Sci. Int.*, vol. 223, no. 1–3, pp. 72–77, 2012, doi: 10.1016/j.forsciint.2012.08.003.

[9] S. Cadd, B. Li, P. Beveridge, W. T. O'Hare, and M. Islam, "Age determination of blood-stained fingerprints using visible wavelength reflectance hyperspectral imaging," *J. Imaging*, vol. 4, no. 12, pp. 5–13, 2018, doi: 10.3390/jimaging4120141.

[10] G. Edelman, V. Manti, S. M. Van Ruth, T. Van Leeuwen, and M. Aalders, "Identification and age estimation of blood stains on colored backgrounds by near infrared spectroscopy," *Forensic Sci. Int.*, vol. 220, no. 1–3, pp. 239–244, 2012, doi: 10.1016/j.forsciint.2012.03.009.

[11] Yang, J., Mathew, J., Dube, R. e Messinger, D., “Spectral feature characterization methods for blood stain detection in crime scene backgrounds”, 2016, 98400E.

[12] H. Lin, Y. Zhang, Q. Wang, B. Li, P. Huang, and Z. Wang, “Estimation of the age of human bloodstains under the simulated indoor and outdoor crime scene conditions by ATR-FTIR spectroscopy,” *Sci. Rep.*, vol. 7, no. 1, pp. 1–9, 2017, doi: 10.1038/s41598-017-13725-1.

[13] G. J. Edelman, E. Gaston, T. G. van Leeuwen, P. J. Cullen, and M. C. G. Aalders, “Hyperspectral imaging for non-contact analysis of forensic traces,” *Forensic Sci. Int.*, vol. 223, no. 1–3, pp. 28–39, 2012, doi: 10.1016/j.forsciint.2012.09.012.

[14] G. Lu and B. Fei, “Medical hyperspectral imaging: a review,” *J. Biomed. Opt.*, vol. 19, no. 1, p. 010901, 2014, doi: 10.1117/1.jbo.19.1.010901.

[15] G. Edelman, *Spectral analysis of blood stains at the crime scene*. 2014.

[16] Li, B.; Beveridge, P.; O’Hare, W.T.; Islam, M. “The estimation of the age of a blood stain using reflectance spectroscopy with a microspectrophotometer, spectral pre-processing and linear discriminant analysis,” *Forensic Sci. Int*. 2011, 212, 198–204.

[17] Janchaysang, S.; Sumriddetchkajorn, S.; Buranasiri, P. “Tunable filter-based multispectral imaging for detection of blood stains on construction material substrates Part 1: Developing blood stain discrimination criteria,” *Appl. Opt*. 2012, 51, 6984–6996.

[18] Janchaysang, S.; Sumriddetchkajorn, S.; Buranasiri, P. “Tunable filter-based multispectral imaging for detection of blood stains on construction material substrates Part 2: Realization of rapid blood stain detection,” *Appl. Opt*.2013, 52, 4898–4910.

[19] Li, B.; Beveridge, P.; O’Hare,W.T.; Islam, M. “The age estimation of blood stains up to 30 days old using visible wavelength hyperspectral image analysis and linear discriminant analysis,” *Sci. Justice* 2013, 53, 270–277.

[20] Li, B.; Beveridge, P.; O’Hare, W.T.; Islam, M. “The application of visible wavelength reflectance hyperspectral imaging for the detection and identification of blood

stains," *Sci. Justice* 2014, 54, 432–438.

[21] Cadd, S.; Li, B.; Beveridge, P.; O'Hare, W.T.; Campbell, A.; Islam, M. "The non-contact detection and identification of blood stained fingerprints using visible wavelength reflectance hyperspectral imaging: Part 1," *Sci. Justice* 2016, 56, 181–190.

[22] Cadd, S.; Li, B.; Beveridge, P.; O'Hare, W.T.; Campbell, A.; Islam, M. "The non-contact detection and identification of blood stained fingerprints using visible wavelength hyperspectral imaging: Part II effectiveness on a range of substrates," *Sci. Justice* 2016, 56, 191–200.

[23] Schuler, R.L.; Kish, P.E.; Plese, C.A. "Preliminary observations on the ability of hyperspectral imaging to provide detection and visualization of bloodstain patterns on black fabrics," *J. Forensic Sci*. 2012, 57, 1562–1569.

[24] B. Li, P. Beveridge, W. T. O'Hare, and M. Islam, "The application of visible wavelength reflectance hyperspectral imaging for the detection and identification of blood stains," *Sci. Justice*, vol. 54, no. 6, pp. 432–438, 2014, doi: 10.1016/j.scijus.2014.05.003.

[25] K. Książek, M. Romaszewski, P. Głomb, B. Grabowski, and M. Cholewa, "Blood stain classification with hyperspectral imaging and deep neural networks," *Sensors (Switzerland)*, vol. 20, no. 22, pp. 1–24, 2020, doi: 10.3390/s20226666.

[26] Che cos'è l'analisi iperspettrale? - Spiegato

[27] J. Zwinkels, "Light, Electromagnetic Spectrum," *Encycl. Color Sci. Technol.*, pp. 1–8, 2015, doi: 10.1007/978/-3-642-27851-8 204-1.

[28] G. J. J. Verhoeven, "The reflection of two fields – Electromagnetic radiation and its role in (aerial) imaging", *AARGnews*, no. 55, pp. 10-18, 2018, doi: 105281/zenodo.3534245.

[29] R.D. Overheim, D.L. Wagner, "Light and Color", United States of America, Wiley, 1992, ISBN: 0-471-08348-8.

[30] Z. M. Khoshhesab, “Reflectance IR Spectroscopy,” *Infrared Spectrosc. - Mater. Sci. Eng. Technol.*, 2012, doi: 10.5772/37180.

[31] Introduction to Spectroscopy.pdf (su.se)

[32] Absorption of Light | Facts, Summary & Definition | Chemistry Revision (alevelchemistry.co.uk)

[33] H. Hellman, “U. S. ATOMIC ENERGY COMMISSION/Dlvislon of Technical Information,” pp. 1–68, 1968.

[34] OP-TEC, “Basics of Spectroscopy: Photonics-Enabled Technologies,” *University of Central Florida,* 2008, ISBN: 1-57837-201-0.

[35] EIU Astro | musings from a physics prof (wordpress.com)

[36] Absorption Spectroscopy - What is Absorption Spectroscopy (ibsen.com).

[37] F. M. Mirabella, “Modern Techniques in Applied Molecular Spectroscopy,” United States of America, Wiley, 1998, ISBN: 0-471-12359-5.

[38] Randall B. Smith, “Introduction to Hyperspectral imaging,” 2012.

Tutorial: Introduction to Hyperspectral Imaging (microimages.com)

[39] Diffuse Reflectance Spectroscopy (DRS) | Division of Atomic Physics (lu.se)

[40] R. Schlögl, “Diffuse Reflectance,” *Catal. from A to Z*, 2020, doi: 10.1002/9783527809080.cataz05336.

[41] Beer Lambert Law | Transmittance & Absorbance | Edinburgh Instruments (edinst.com).

[42] M. West, J. Grossmann, and C. Galvan, “Commercial Snapshot Spectral Imaging: The Art of the Possible,” no. September 2018, 2018.

[43] D.L. Exline, C. Wallace, C. Roux, C. Lennard, M.P. Nelson, P.J. Treado, “Forensic applications of chemical imaging: latent fingerprint detection using visible absorption and luminescence,” *J. Forensic Sci*. 48 (2003) 1047–1053.

[44] G. Payne, B. Reedy, C. Lennard, B. Comber, D. Exline, C. Roux, “A further study to

investigate the detection and enhancement of latent fingerprints using visible absorption and luminescence chemical imaging," *Forensic Sci. Int*. 150 (2005) 33–51.

[45] K.S. Kalasinsky, J. Magluilo Jr., T. Schaefer, "Hair analysis by infrared microscopy for drugs of abuse," *Forensic Sci. Int.* 63 (1993) 253–260.

[46] What are Neural Networks? | IBM

[47] S. Sharma, S. Sharma, and A. Athaiya, "Activation Functions in Neural Networks," *Int. J. Eng. Appl. Sci. Technol.*, vol. 04, no. 12, pp. 310–316, 2020, doi: 10.33564/ijeast.2020.v04i12.054.

[48] M. N. Vrahatis, G. D. Magoulas, K. E. Parsopoulos, and V. P. Plagianakos, "Introduction to Artificial Neural Networks and Applications," *Proc. Neurosci. 2000 Conf.*, no. November 2014, pp. 1–12, 2001, doi: 10.13140/2.1.1755.2322.

[49] M. H. SAZLI, "A brief review of feed-forward neural networks," *Commun. Fac. Sci. Univ. Ankara*, no. January 2006, pp. 11–17, 2006, doi: 10.1501/0003168.

[50] S. Haykin. "Neural Networks, A Comprehensive foundation", 2nd edition. Prentice Hall, 1999.

[51] Neural Network Definition | DeepAI

[52] The Essential Guide to Neural Network Architectures (v7labs.com)

[53] About Train, Validation and Test Sets in Machine Learning | by Tarang Shah | Towards Data Science

[54] C.L. Stanfield, "Principles of Human Physiology," San Francisco, Pearson Benjamin Cummings, 5th edition, 2012, ISBN: 0-321-81934-9.

[55] Frontiers | An Introductory Review of Deep Learning for Prediction Models With Big Data | Artificial Intelligence (frontiersin.org).

[56] What is an artificial neuron and why does it need an activation function? | by Bartosz Szabłowski | Towards Data Science.

[57] Gurney, K. “An Introduction to Neural Networks (1st ed.),” *CRC Press,* 1997, https://doi.org/10.1201/9781315273570

[58] P. Castellini, N. Giulietti, N. Falcionelli, A. F. Dragoni, and P. Chiariotti, “a Neural Network Based Approach To Gridless Sound Source Identification,” pp. 1–9, 2020.

[59] Crash Course On Multi-Layer Perceptron Neural Networks (machinelearningmastery.com)

[60] Supervised and unsupervised learning - Neural Networks with Java (nnwj.de)

[61] Supervised vs. Unsupervised Learning: What’s the Difference? | IBM

[62] Elsy Gómez-Ramos & Francisco Venegas-Martínez, "A Review of Artificial Neural Networks: How Well Do They Perform in Forecasting Time Series?," Analítika, Analítika - Revista de Análisis Estadístico/Journal of Statistical Analysis, vol. 6(2), pages 7-15, 2013.

[63] Multilayer Perceptron Explained with a Real-Life Example and Python Code: Sentiment Analysis | by Carolina Bento | Towards Data Science

[64] Mutli-Layer Perceptron - Back Propagation (unsw.edu.au).

[65] S. Sun, Z. Cao, H. Zhu, J. Zhao, “A survey of optimization methods froma machine learning perspective”.

[66] A. J. Marengo-Rowe, “Structure-Function Relations of Human Hemoglobins,” *Baylor Univ. Med. Cent. Proc.*, vol. 19, no. 3, pp. 239–245, 2006, doi: 10.1080/08998280.2006.11928171.

[67] R. H. Bremmer, D. M. de Bruin, M. de Joode, W. J. Buma, T. G. van Leeuwen, and M. C. G. Aalders, “Biphasic oxidation of Oxy-Hemoglobin in bloodstains,” *PLoS One*, vol. 6, no. 7, pp. 1–6, 2011, doi: 10.1371/journal.pone.0021845.

[68] R. H. Bremmer, A. Nadort, T. G. van Leeuwen, M. J. C. van Gemert, and M. C. G. Aalders, “Age estimation of blood stains by hemoglobin derivative determination using reflectance spectroscopy,” *Forensic Sci. Int.*, vol. 206, no. 1–3, pp. 166–171, 2011, doi: 10.1016/j.forsciint.2010.07.034.

[69] B. Li, P. Beveridge, W. T. O'Hare, and M. Islam, "The age estimation of blood stains up to 30 days old using visible wavelength hyperspectral image analysis and linear discriminant analysis," *Sci. Justice*, vol. 53, no. 3, pp. 270–277, 2013, doi: 10.1016/j.scijus.2013.04.004.

[70] HinaLea Imaging, "User Manual: Model 4250 VNIR 4250 System Technical Specifications".
VNIR-4250-Intelligent-Imaging-System-0720-F2.pdf (hinaleaimaging.com)

[71] J. H. Stock, M. W. Watson, "Introduzione all'econometria," *Pearson Italia Spa*, 2005.

[72] A Conceptual Explanation of Bayesian Hyperparameter Optimization for Machine Learning | by Will Koehrsen | Towards Data Science.

[73] T. Agrawal, Bayesian optimization, Hyperparameter Optimization in Machine Learning (2020) 81–108doi:10.1007/978-1-4842-6579-6_4.

[74] Ottimizzazione delle reti neurali profonde tramite l'ottimizzazione degli iperparametri. (ichi.pro)

[75] Mean Percentage Error Formula: A Statistical Analysis | Total Assignment Help.

[76] Standard Deviation Definition (investopedia.com)

[77] Variance Definition (investopedia.com)

[78] What is Standard Deviation? Definition of Standard Deviation, Standard Deviation Meaning - The Economic Times (indiatimes.com)

[80] Temperature of a Halogen Light Bulb - The Physics Factbook (hypertextbook.com)
https://hypertextbook.com/facts/2003/ElaineDevora.shtml

[81] C. D. Elvidge, D. M. Keith, B. T. Tuttle, and K. E. Baugh, "Spectral identification of lighting type and character," *Sensors*, vol. 10, no. 4, pp. 3961–3988, 2010, doi: 10.3390/s100403961.

[82] W.J. Moses, J.H. Bowles, R.L. Lucke, and M.R. Corson, “Impact of signal-to-noise ratio in a hyperspectral sensor on the accuracy of biophysical parameter estimation in case II waters,” *National Research Council/Naval Research Laboratory Research Associate, Washington, D.C., USA Naval Research Laboratory, Washington, D. C., USA,* 2012.

[83] B. Rasti, P. Scheunders, P. Ghamisi, G. Licciardi, and J. Chanussot, “Noise reduction in hyperspectral imagery: Overview and application,” *Remote Sens.*, vol. 10, no. 3, pp. 1–28, 2018, doi: 10.3390/rs10030482.

[84] J. G. Chicco D, Warrens MJ, “The coefficient of determination r-squared is more informative than smape, mae, mape, mse and rmse in regression analysis evaluation,” doi:https://doi.org/10.7717/peerj-cs.623.

[85] G. McLaughlin, V. Sikirzhytski, I. K. Lednev, “Circumventing substrate interference in the raman spectroscopic identification of blood stains,” *Forensic Science International* 231 (1-3) (2013) 157–166. doi:10.1016/ j.forsciint.2013.04.033.